Electronic Supplementary Material (ESI) for Dalton Transactions.

SUPPORTING INFORMATION

Pd(II)/diphosphine/curcumin complexes as potential anticancer agents

Jocely L. Dutra,*[a,b] João Honorato,[c] Angélica Graminha,[a] Carlos André F. Moraes,[a] Kleber T. de Oliveira,[a] Marcia R. Cominetti,[d] Eduardo E. Castellano[e] and Alzir A. Batista*[a]

a. Departamento de Química, Universidade Federal de São Carlos – UFSCar, CP 676, CEP 13561-901, São Carlos, SP, Brazil. E-mail: jocely.dut@hotmail.com; daab@ufscar.br
b. Departamento de Química, Universidade Federal do Amazonas – UFAM, CEP 69077-000, Itacoatiara, AM, Brazil
c. Instituto de Química, Universidade de São Paulo – USP, CEP 05508-900, São Paulo, SP, Brazil.
d. Departamento de Gerontologia, Universidade Federal de São Carlos – UFSCar, CP 676, 13561-901, São Carlos, SP, Brazil.
e. Instituto de Física de São Carlos, Universidade de São Paulo – USP, CP 369, CEP 13560-970, São Carlos, SP, Brazil.

Characterization of complexes

Figures

Tables

Complexes structure

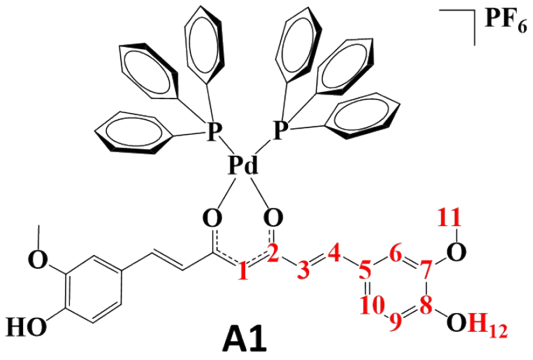

A1

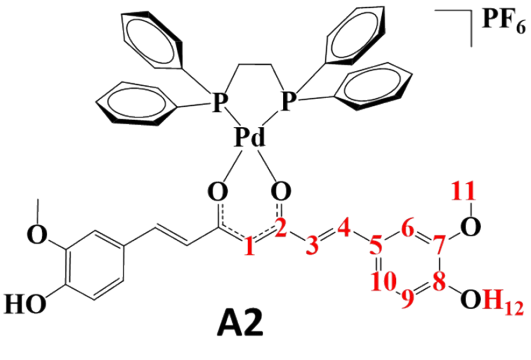

A2

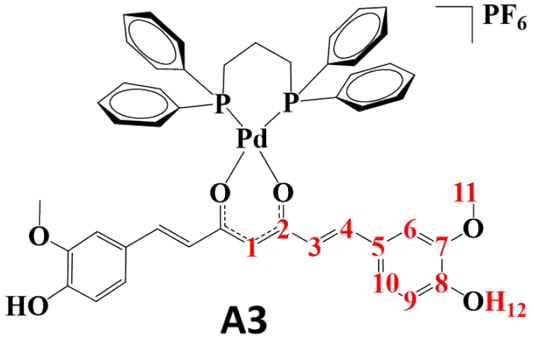

A3

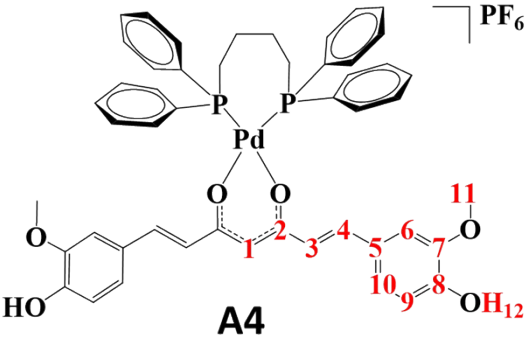

A4

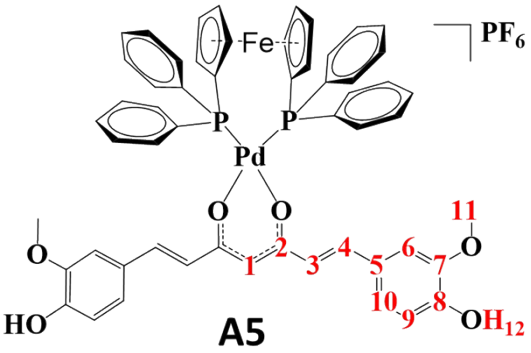

A5

Figures

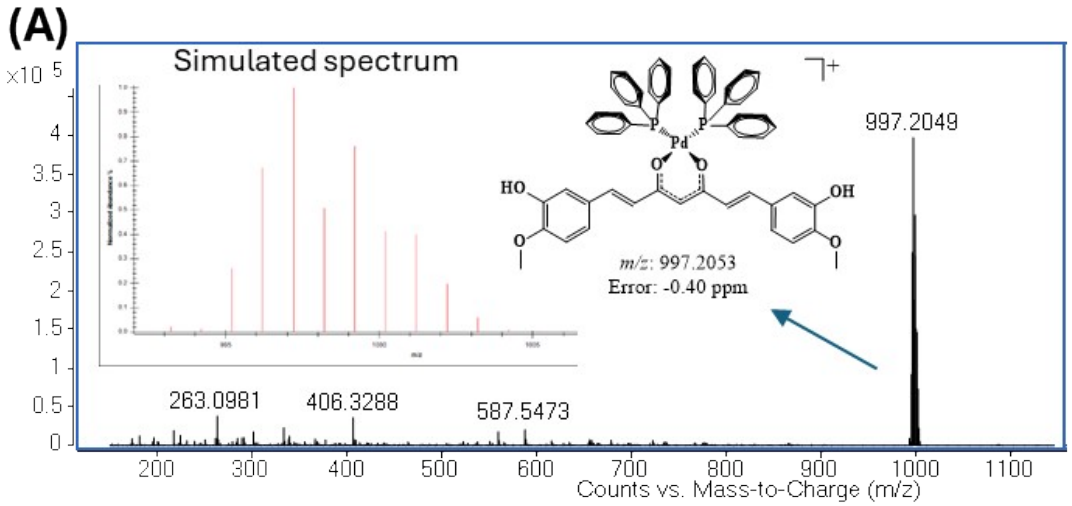
(A)
Simulated spectrum
997.2049
m/z: 997.2053
Error: -0.40 ppm
263.0981
406.3288
587.5473
Counts vs. Mass-to-Charge (m/z)

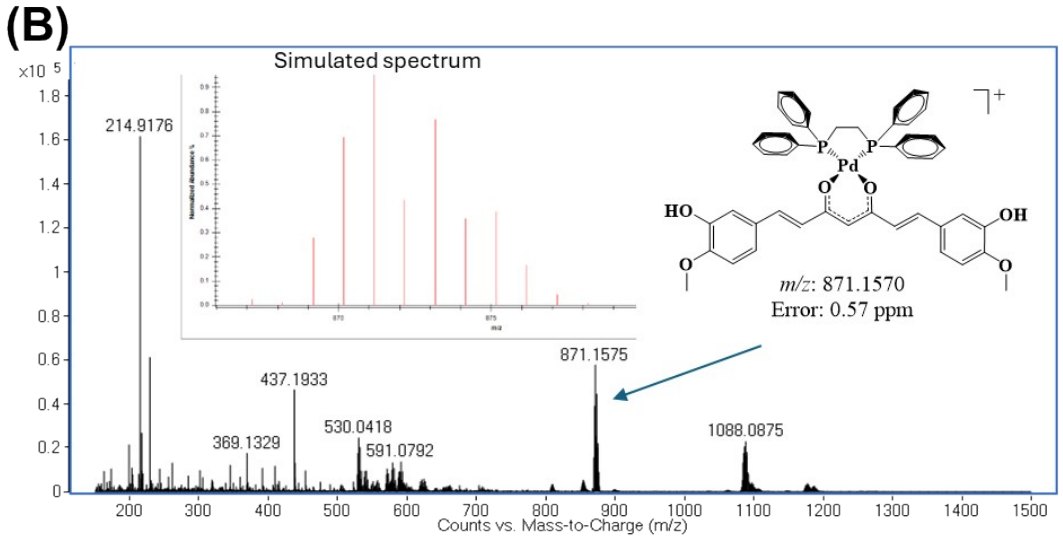
(B)
Simulated spectrum
214.9176
871.1575
437.1933
530.0418
369.1329
591.0792
1088.0875
m/z: 871.1570
Error: 0.57 ppm
Counts vs. Mass-to-Charge (m/z)

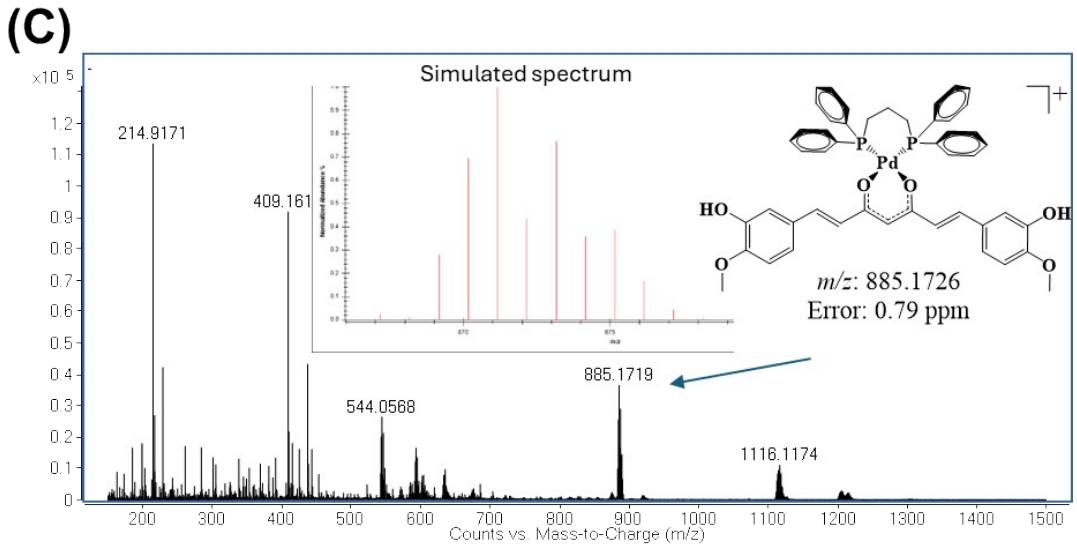
(C)
Simulated spectrum
214.9171
409.161
885.1719
544.0568
1116.1174
m/z: 885.1726
Error: 0.79 ppm
Counts vs. Mass-to-Charge (m/z)

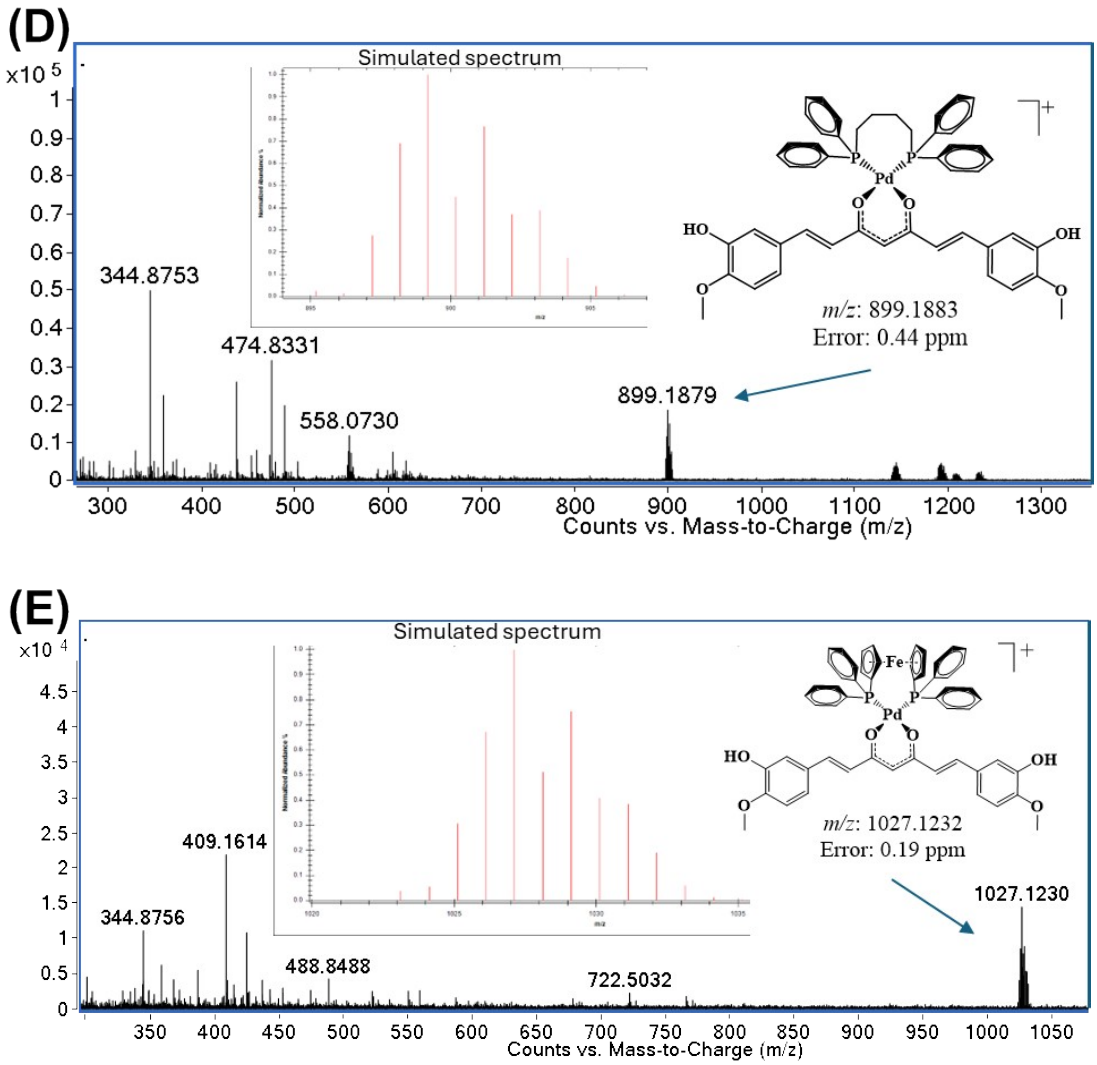

Figure S1. ESI(+)-MS/MS analysis of the complexes (A) *A1*, (B) *A2*, (C) *A3*, (D) *A4* e (E) *A5*. Comparison between theoretical and experimental mass isotope distribution corresponding to the $[M]^+$.

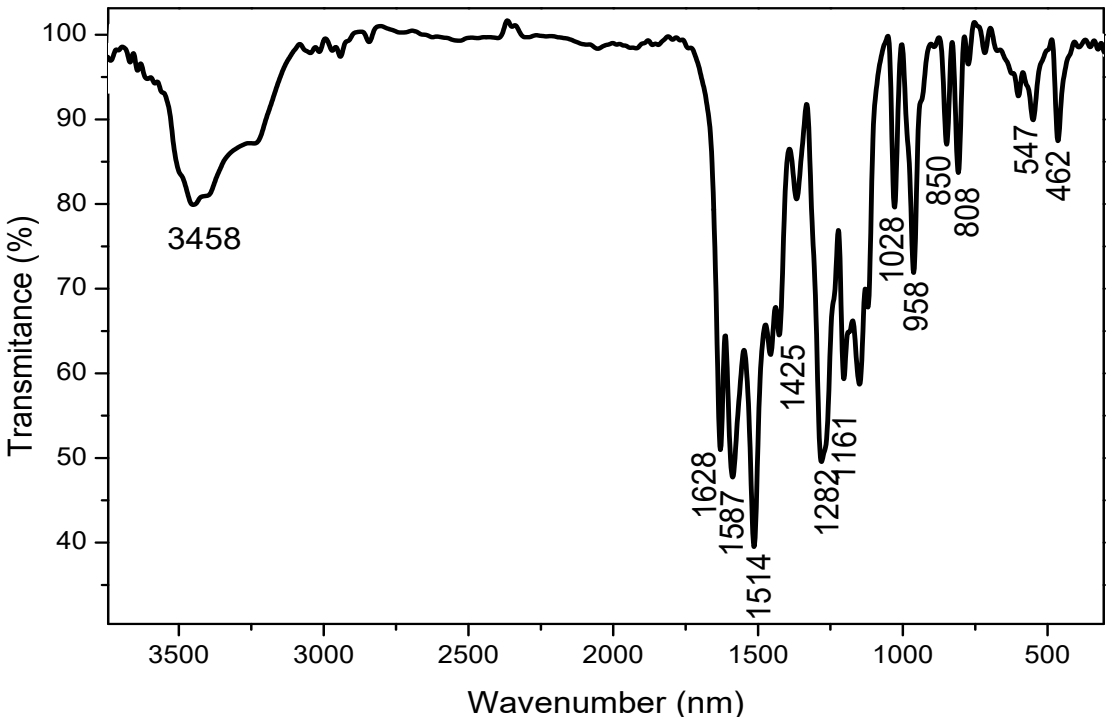

Figure S2. FTIR spectra for the curcumin.

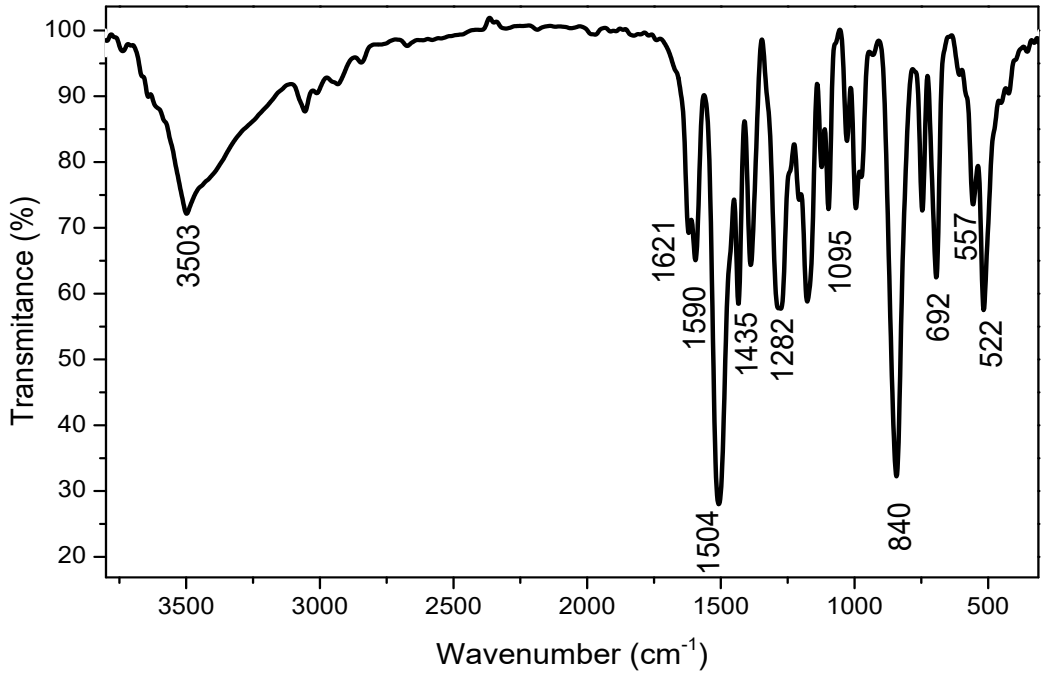

Figure S3. FTIR spectra for complex **A1**.

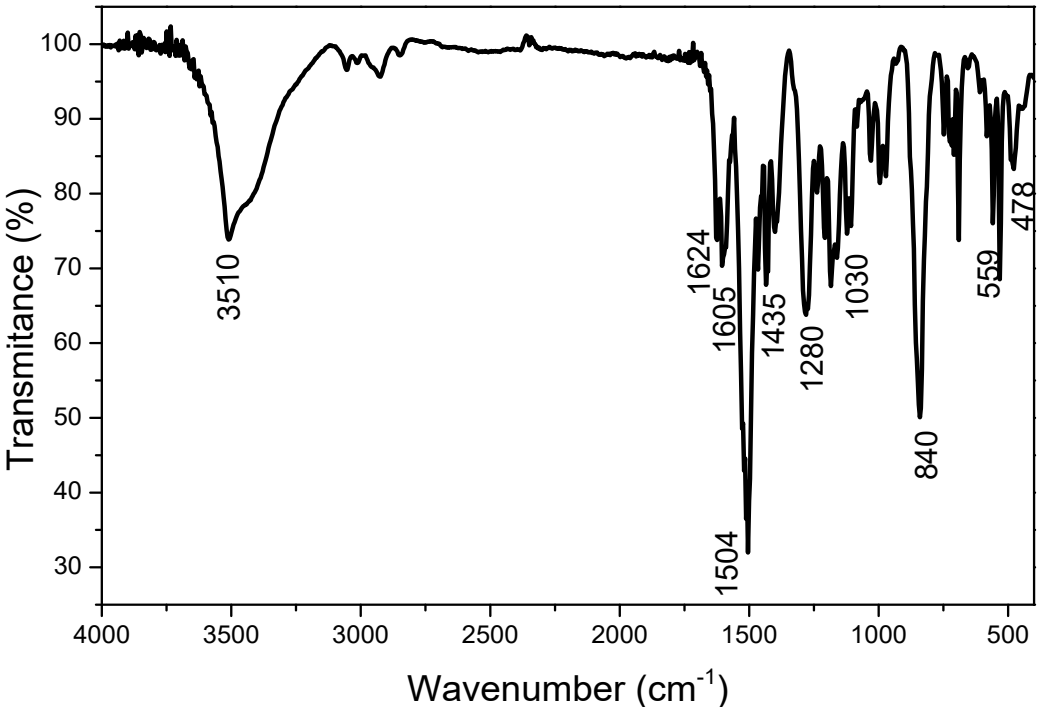

Figure S4. FTIR spectra for complex **A2.**

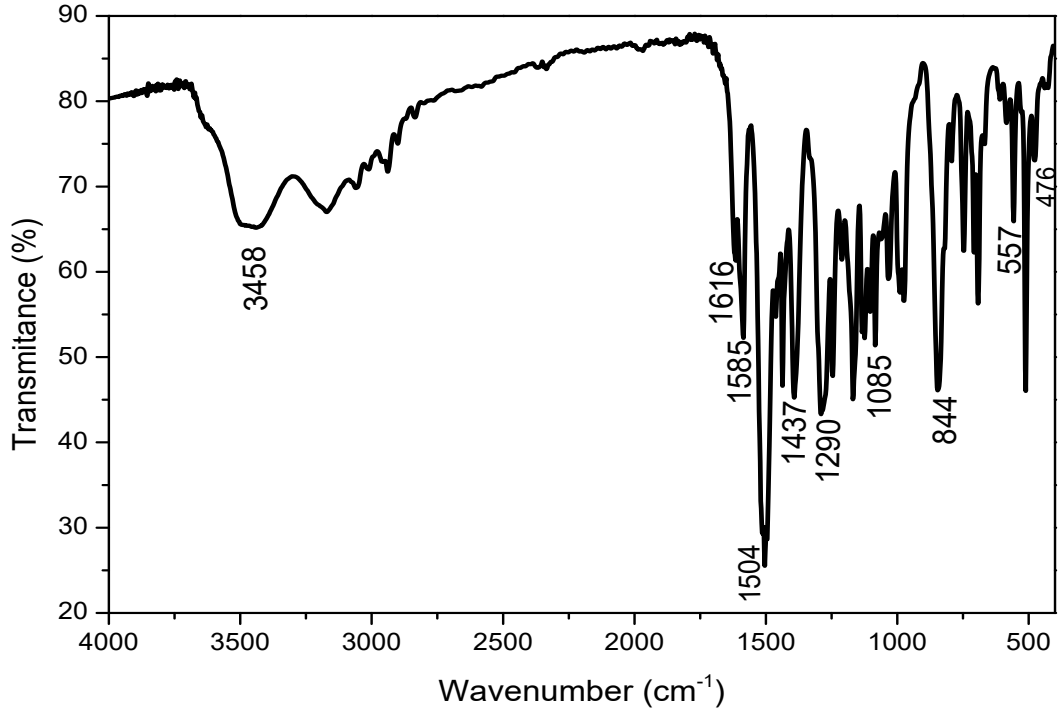

Figure S5. FTIR spectra for complex *A3*.

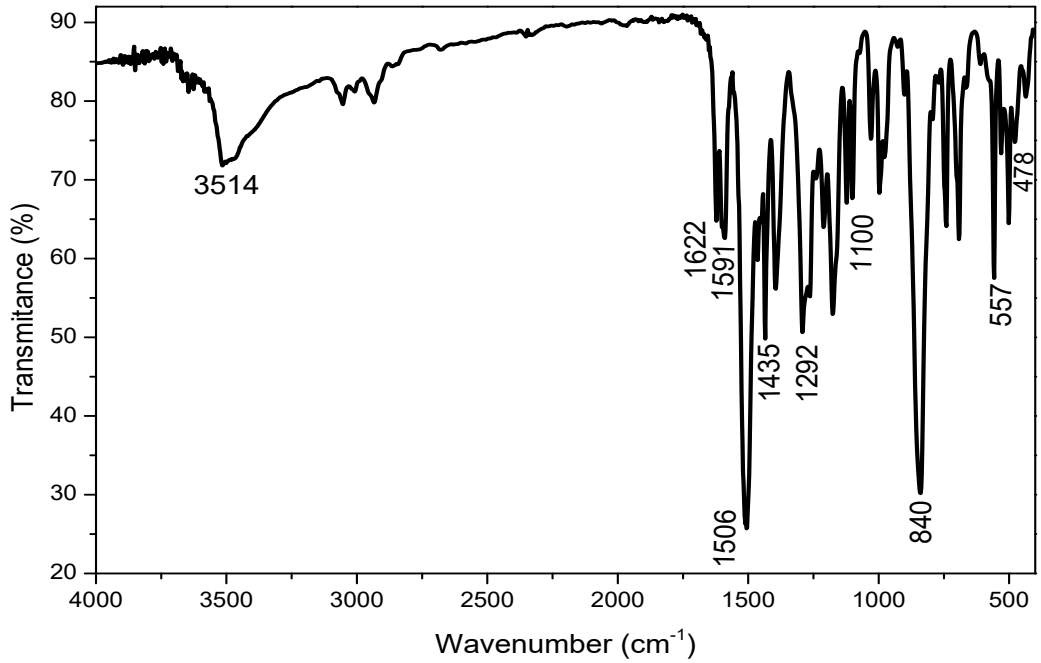

Figure S6. FTIR spectra for complex *A4*.

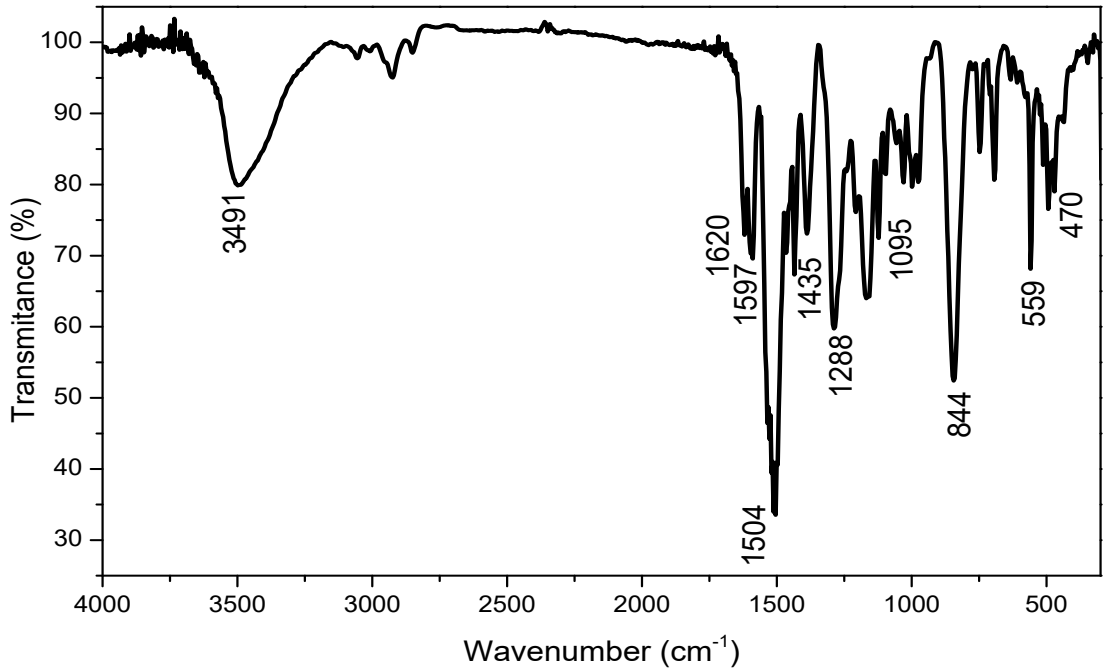

Figure S7. FTIR spectra for complex *A5*.

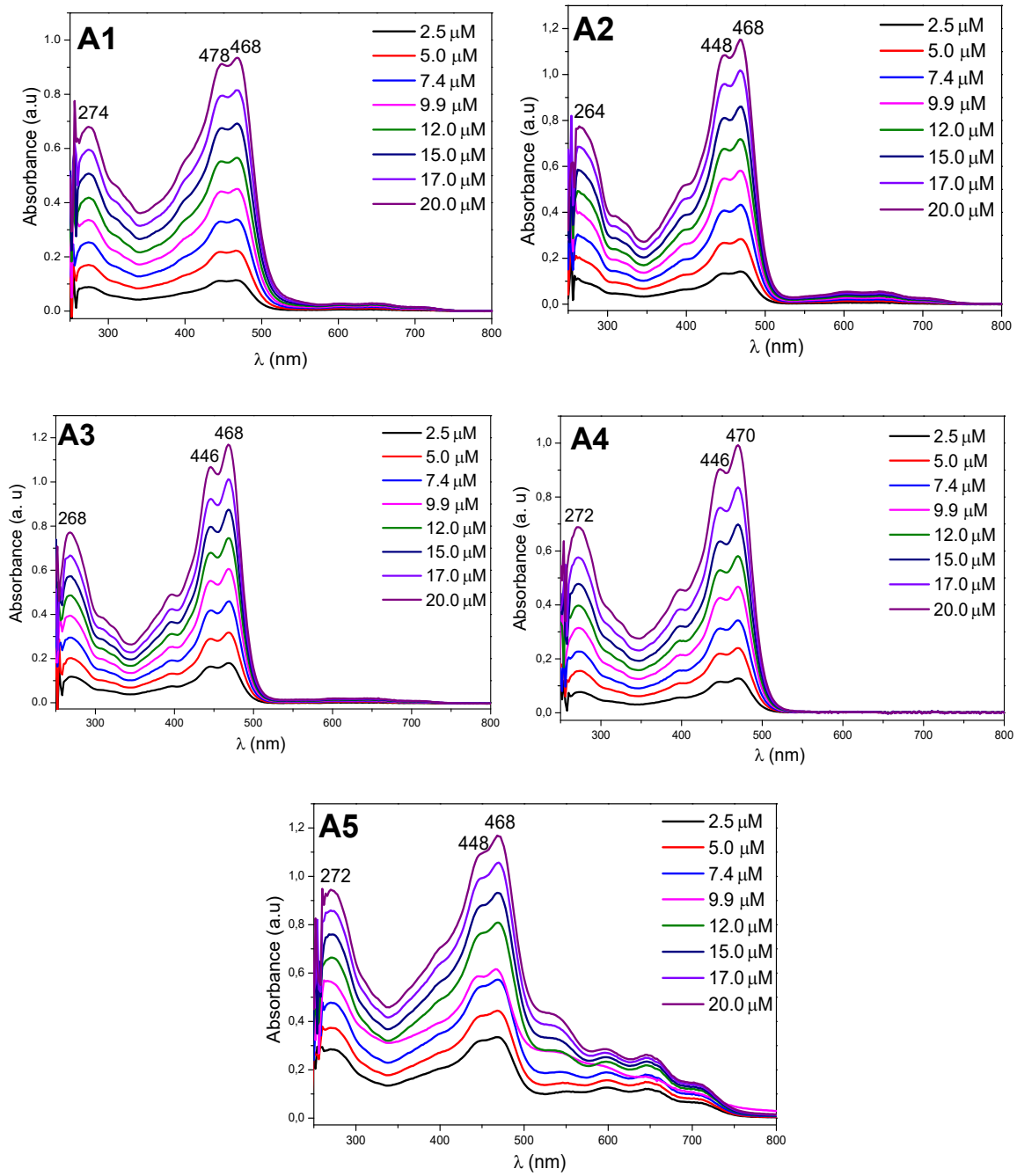

Figure S8. UV-vis spectra of the complexes *A1-A5* in DMSO.

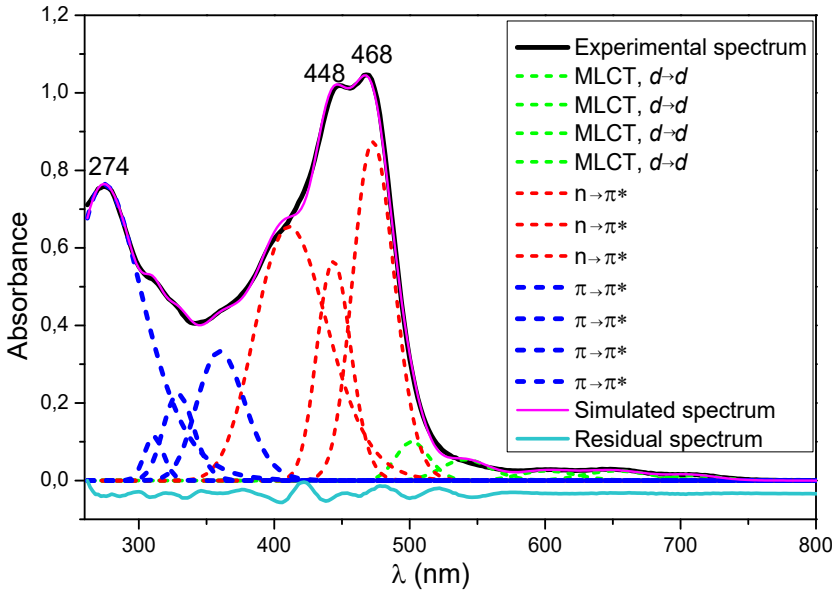

Figure S9. UV-vis spectrum of complex *A1* deconvoluted in Matlab.

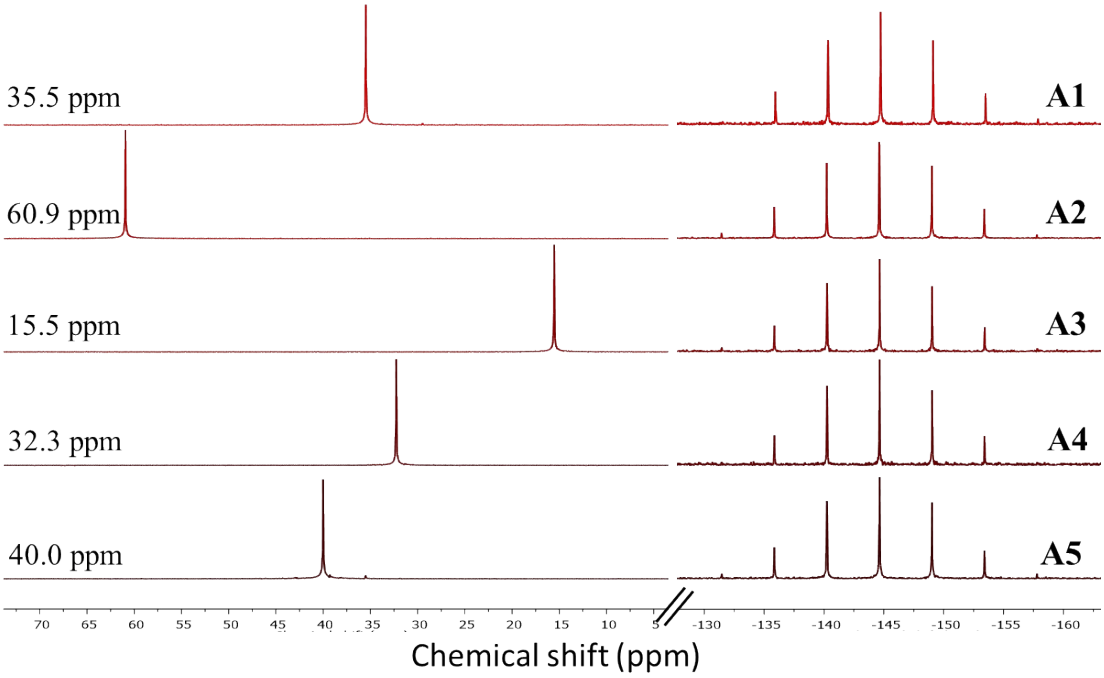

Figure S10. $^{31}P\{^{1}H\}$ NMR spectra of complexes *A1–A5*, in CH_2Cl_2 (with D_2O capillary).

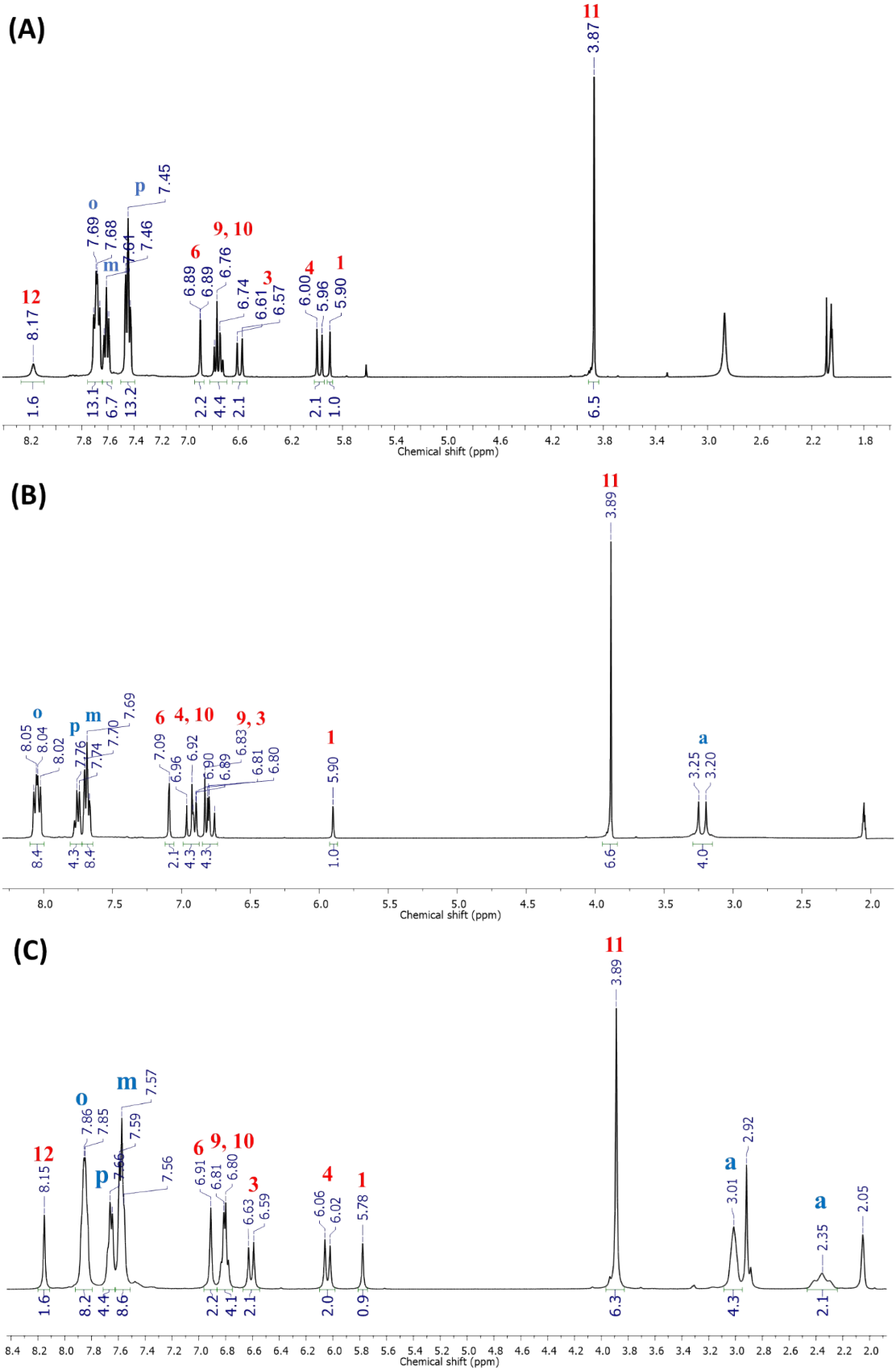
(A)
11
3.87
p
7.45
o
7.69
7.68
7.61
7.46
m
9, 10
6
6.89
6.89
6.76
6.74
3
6.61
6.57
4
6.00
5.96
1
5.90
12
8.17
1.6
13.1
6.7
13.2
2.2
4.4
2.1
2.1
1.0
6.5
Chemical shift (ppm)
(B)
11
3.89
o
8.05
8.04
8.02
p
7.76
7.74
m
7.70
7.69
6
7.09
6.96
4, 10
6.92
6.90
6.89
9, 3
6.83
6.81
6.80
1
5.90
a
3.25
3.20
8.4
4.3
8.4
2.1
4.3
4.3
1.0
6.6
4.0
Chemical shift (ppm)
(C)
11
3.89
m
7.57
o
7.86
7.85
7.59
12
8.15
p
7.66
7.56
6
6.91
6.81
6.80
9, 10
3
6.63
6.59
4
6.06
6.02
1
5.78
a
3.01
2.92
a
2.35
2.05
1.6
8.2
4.4
8.6
2.2
4.1
2.1
2.0
0.9
6.3
4.3
2.1
Chemical shift (ppm)

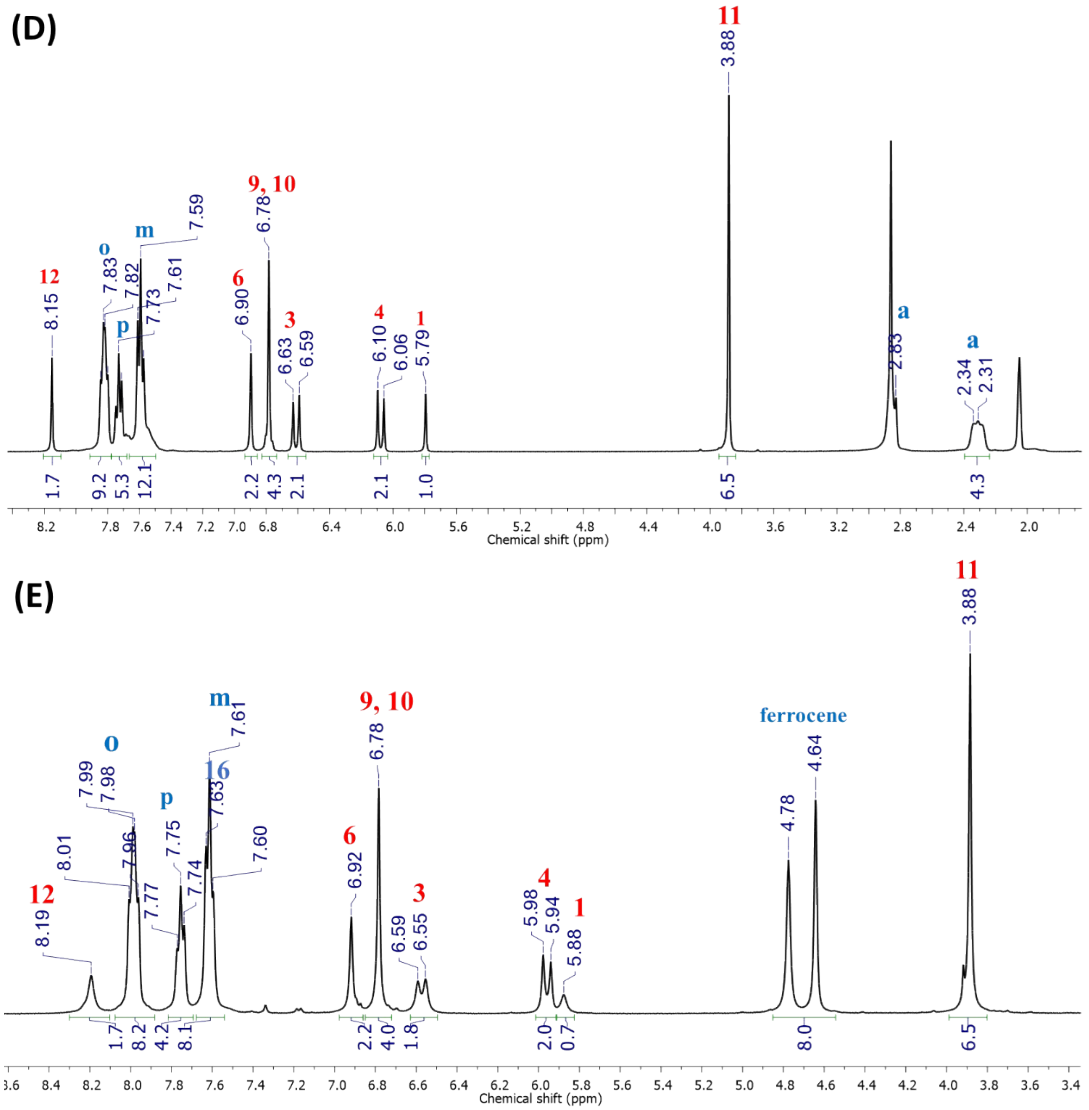

Figure S11. NMR ^{1}H spectra of the complexes (A) *A1*; (B) *A2*; (C) *A3*; (D) *A4* e (E) *A5*, in acetone-d_6.

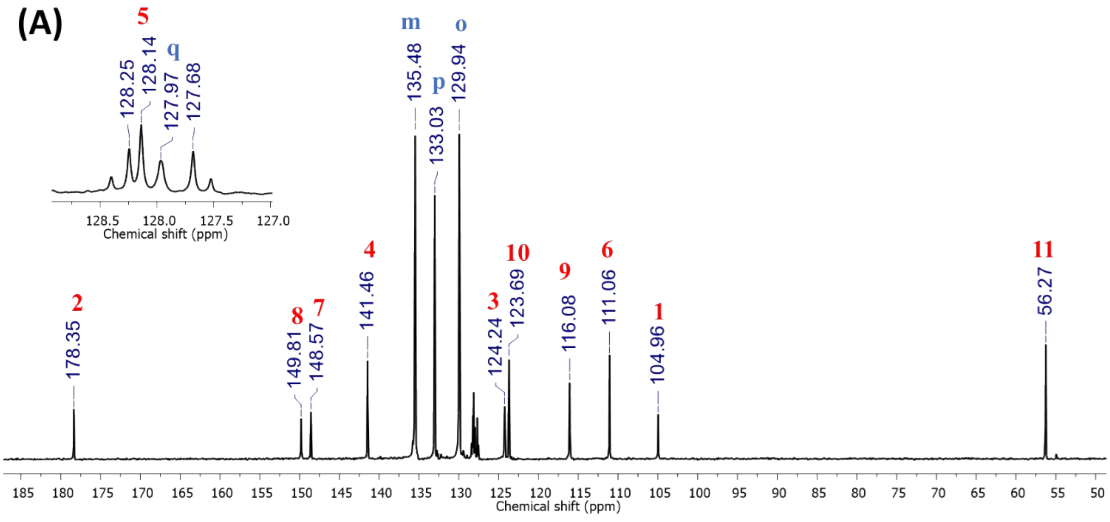

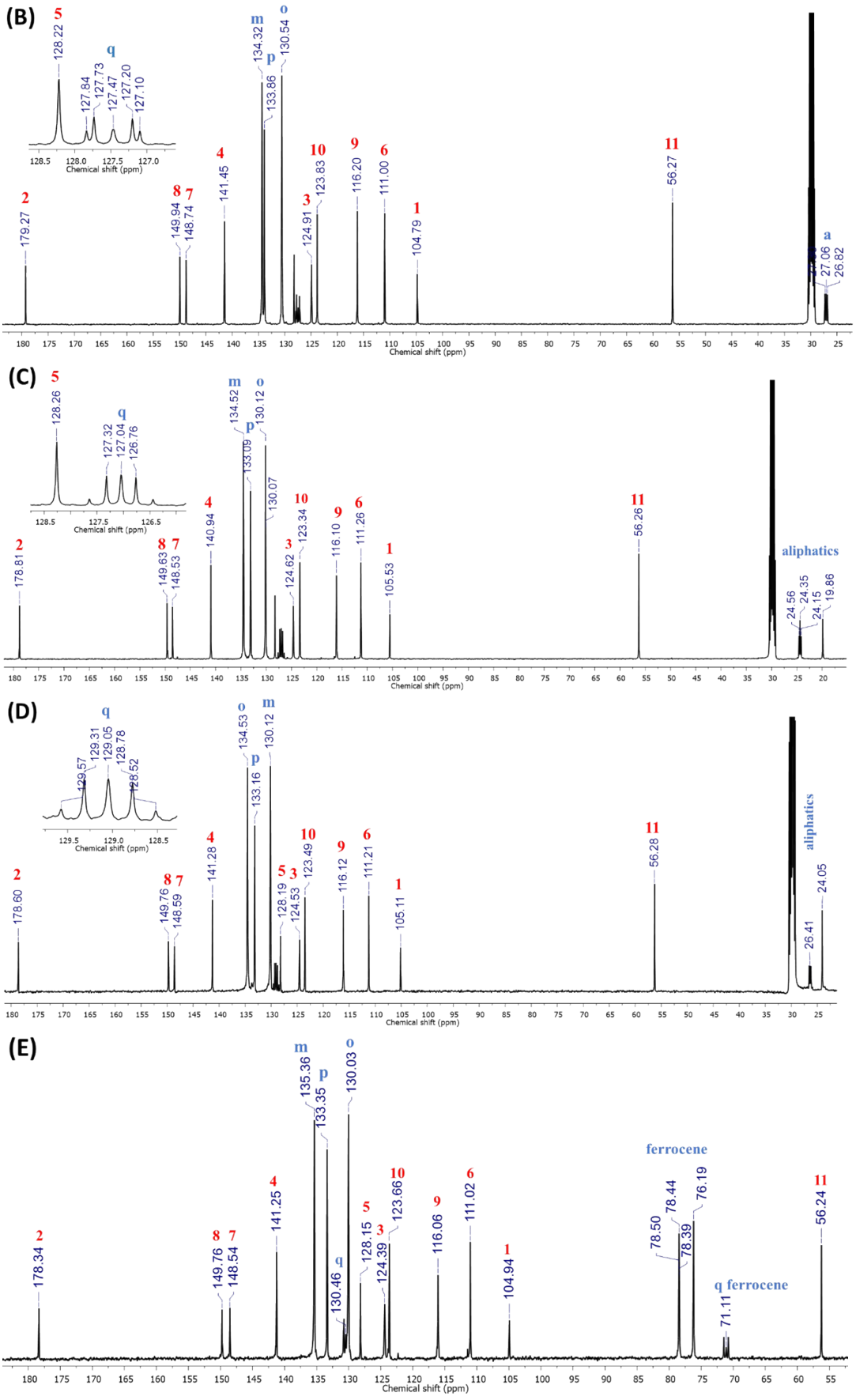

Figure S12. NMR ^{13}C spectra of complexes (A) **A1**; (B) **A2**; (C) **A3;** (D) **A4** and (E) **A5**, in acetone-d_6.

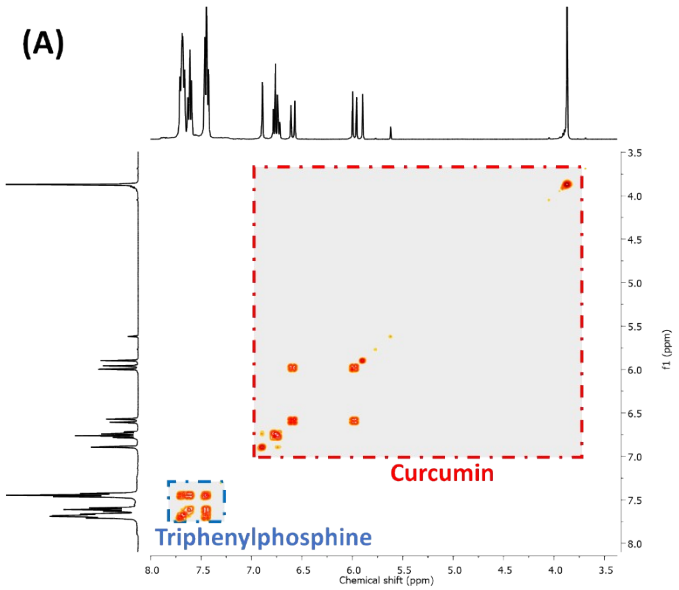
(A)
Curcumin
Triphenylphosphine
f1 (ppm)
Chemical shift (ppm)

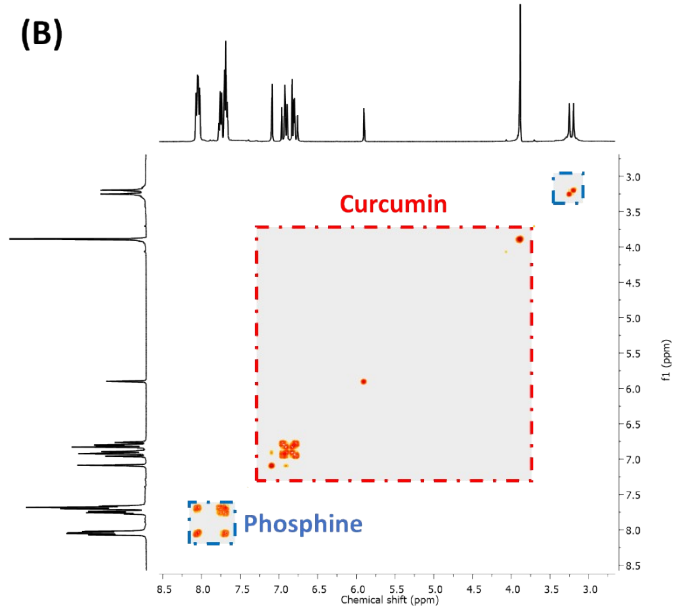
(B)
Curcumin
Phosphine
f1 (ppm)
Chemical shift (ppm)

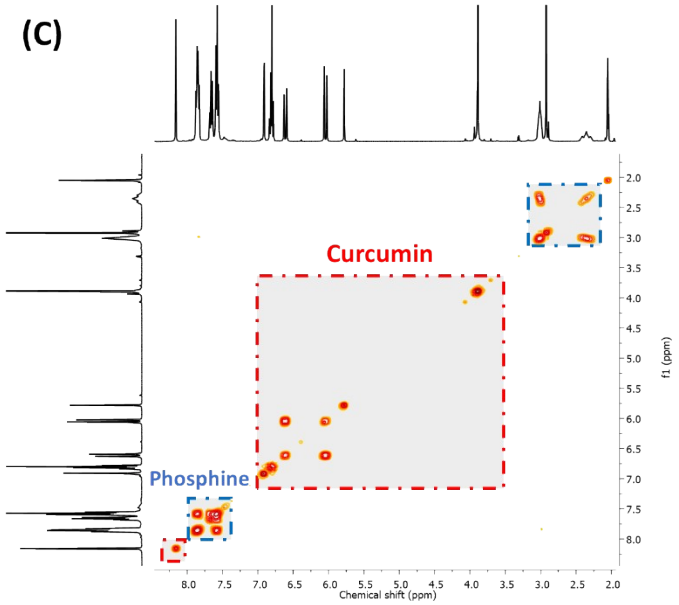
(C)
Curcumin
Phosphine
f1 (ppm)
Chemical shift (ppm)

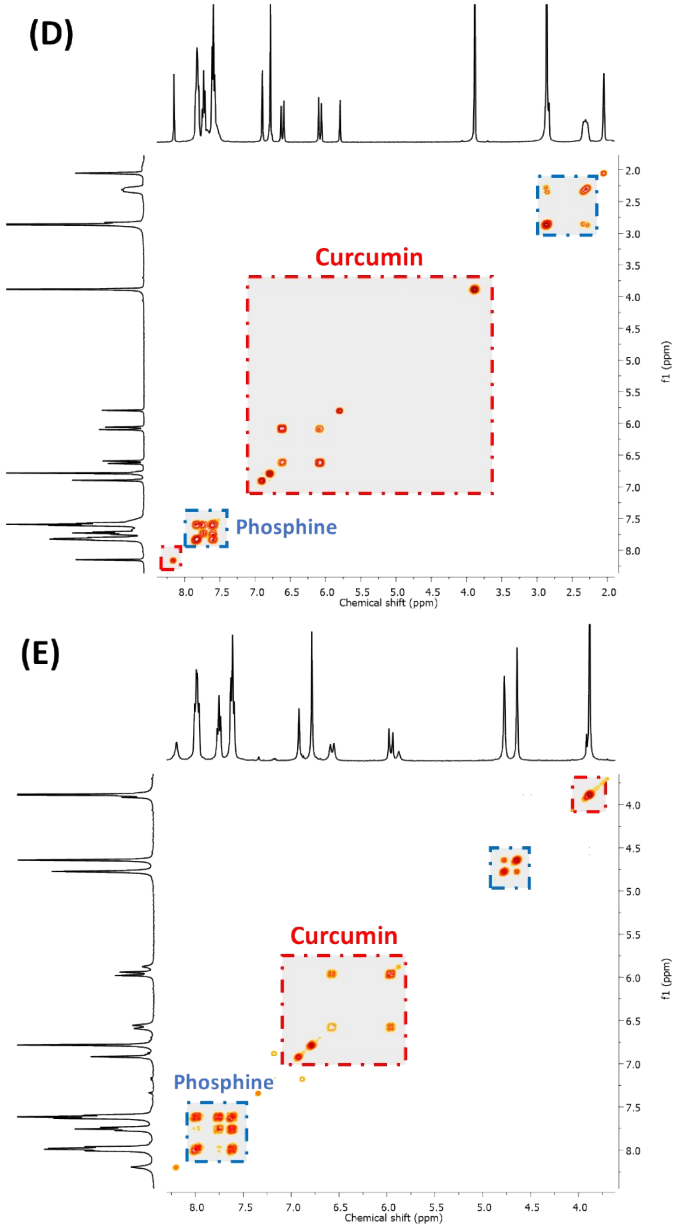

Figure S13. COSY ^{1}H-^{1}H NMR spectra of complexes (A) **A1**; (B) **A2**; (C) **A3;** (D) **A4** and (E) **A5**, in acetone-d_6.

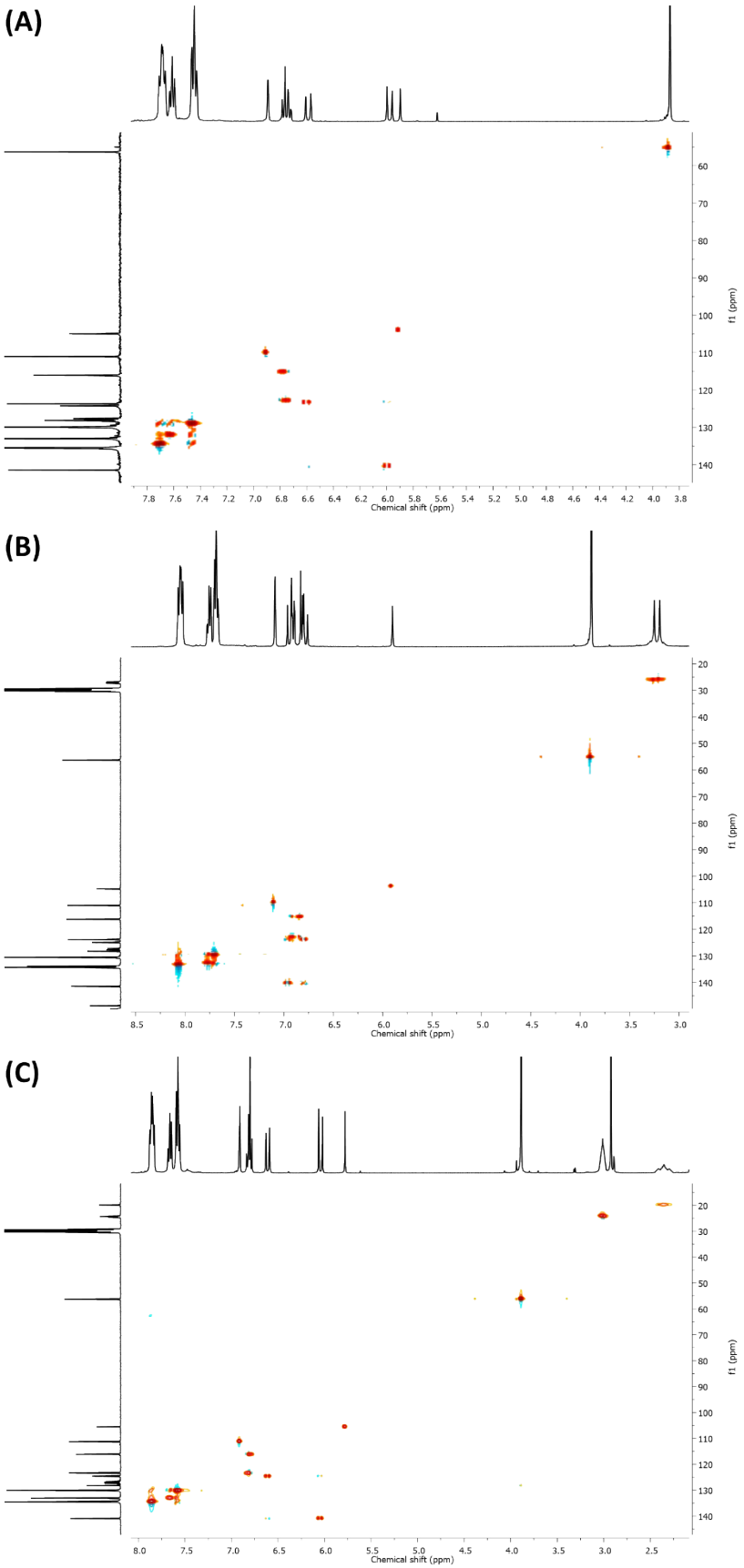
(A)
Chemical shift (ppm)
f1 (ppm)
(B)
Chemical shift (ppm)
f1 (ppm)
(C)
Chemical shift (ppm)
f1 (ppm)

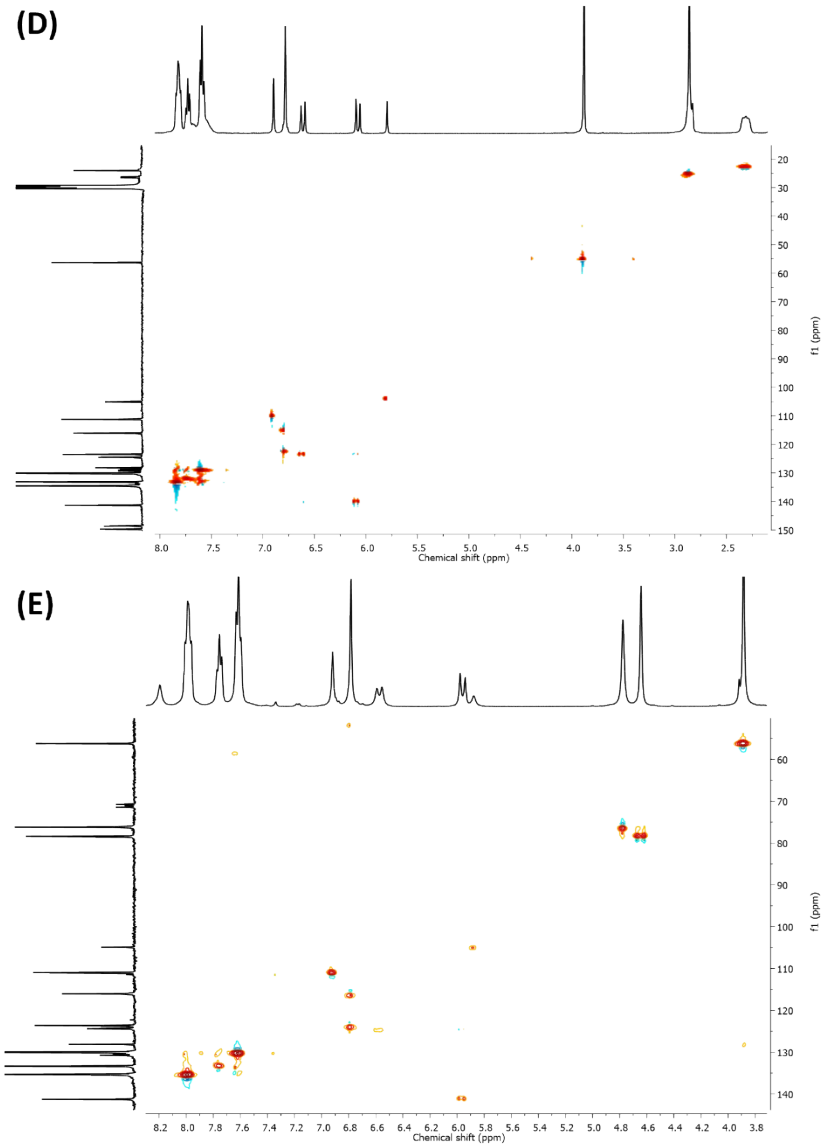

Figure S14. ^{1}H-^{13}C HSQC NMR of complexes (A) **A1**; (B) **A2**; (C) **A3;** (D) **A4** and (E) **A5**, in acetone-d_6.

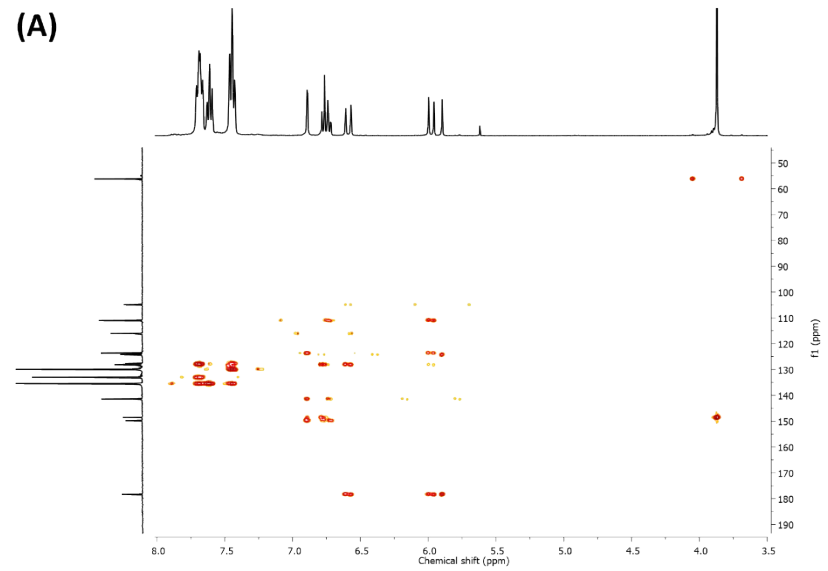

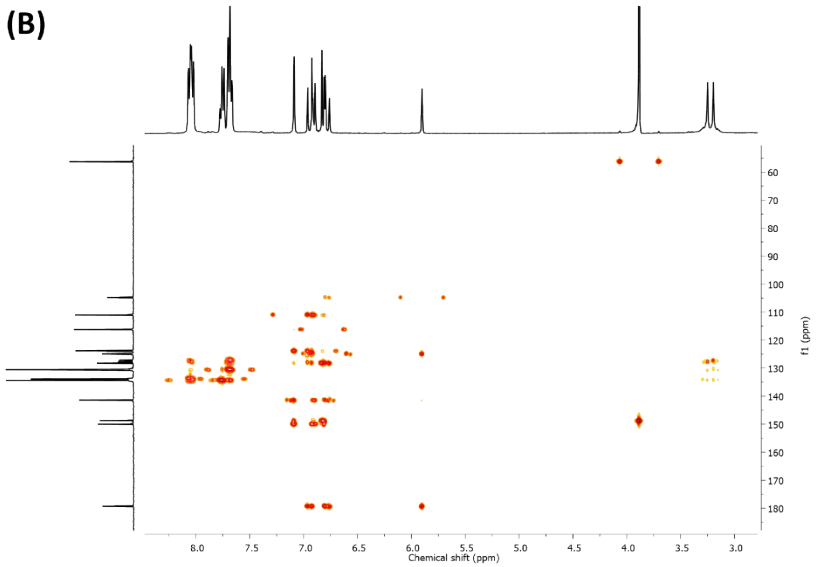
(B)
f1 (ppm)
Chemical shift (ppm)

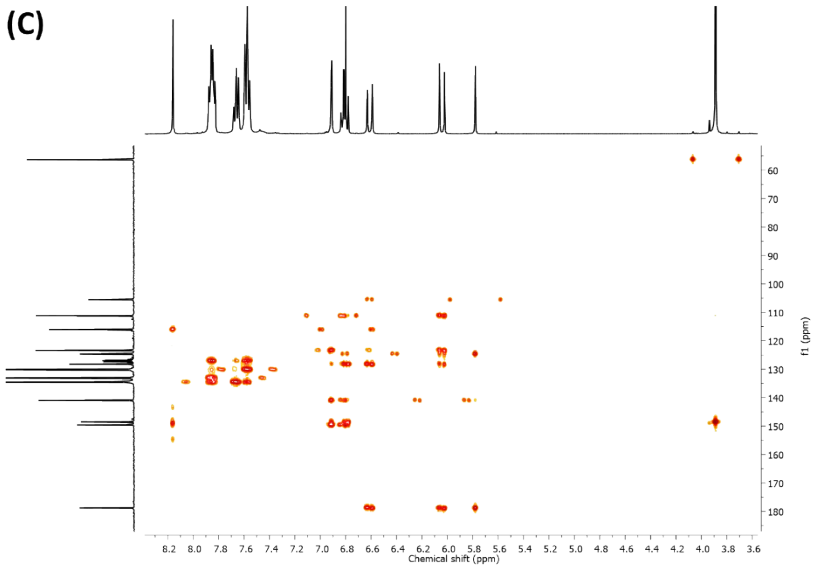
(C)
f1 (ppm)
Chemical shift (ppm)

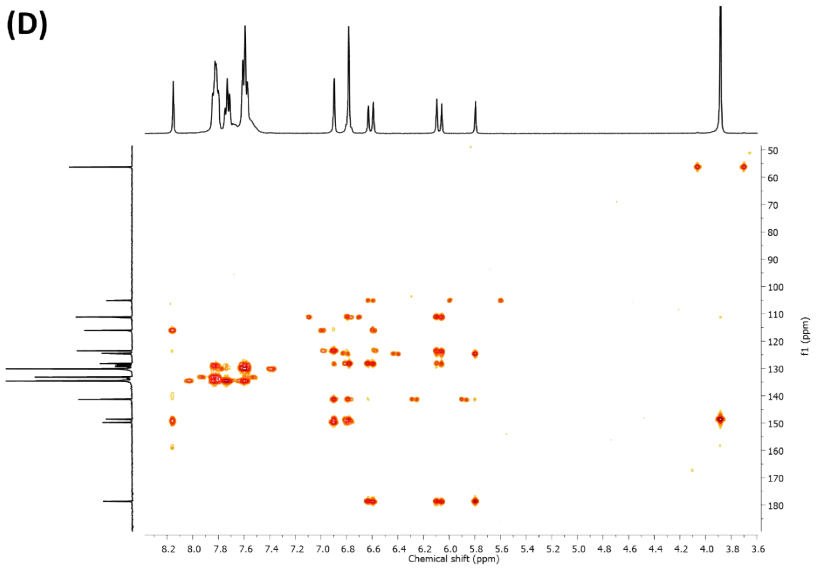
(D)
f1 (ppm)
Chemical shift (ppm)

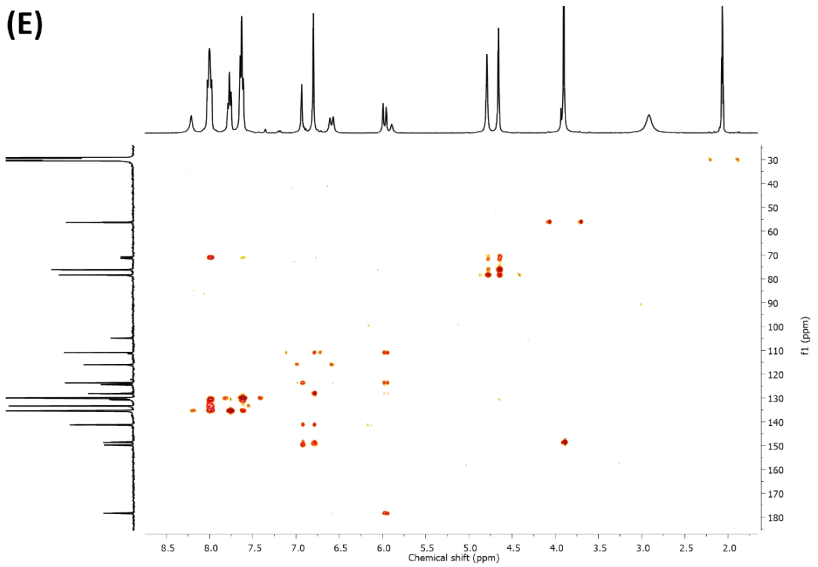

Figure S15. ^{1}H-^{13}C HMBC NMR of complexes (A) **A1**; (B) **A2**; (C) **A3;** (D) **A4** and (E) **A5**, in acetone-d_6.

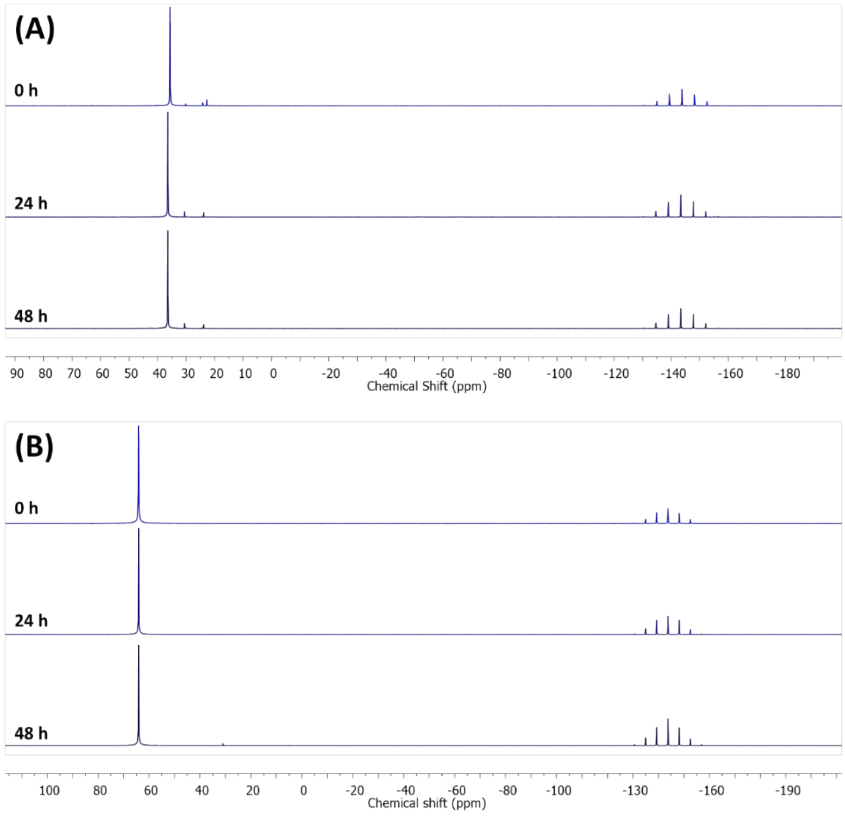

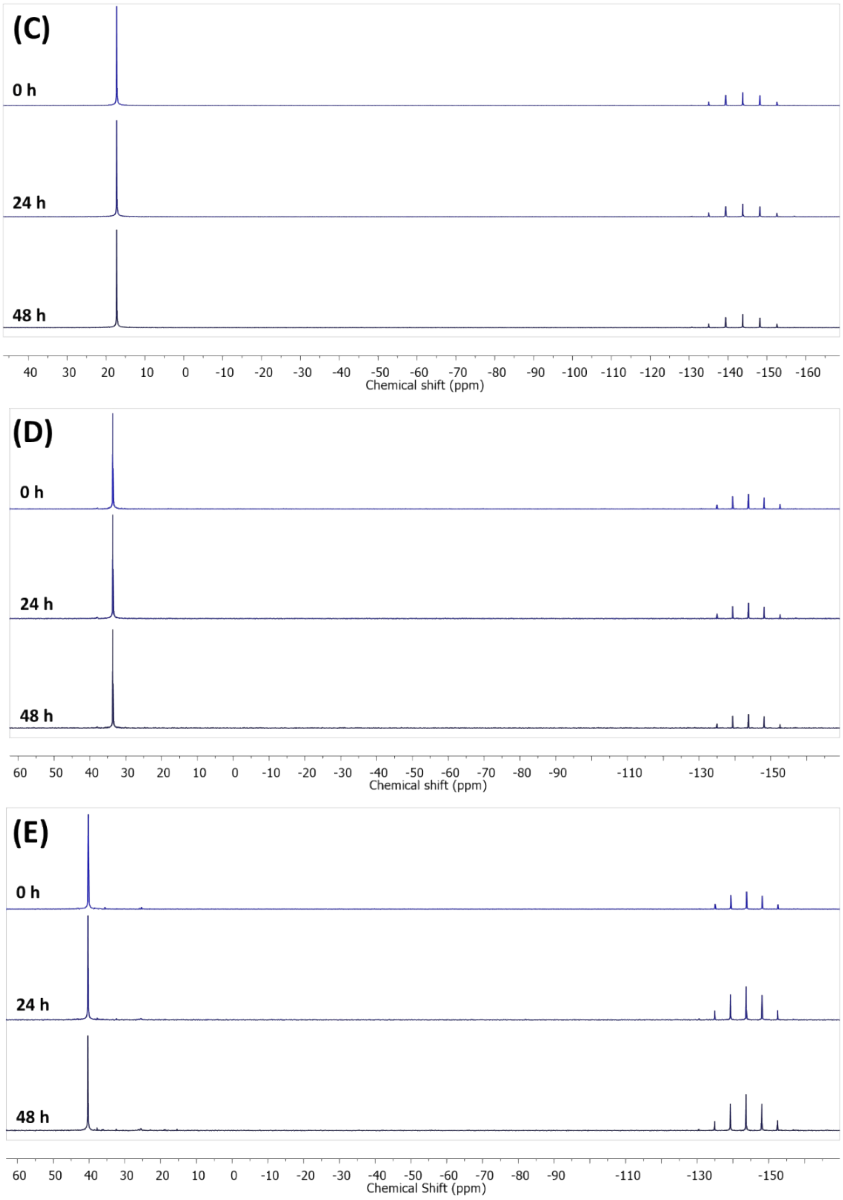

Figure S16. $^{31}P\{^{1}H\}$ NMR spectra of the complexes (A) **A1**; (B) **A2**; (C) **A3;** (D) **A4** and (E) **A5**, in DMSO (with D_2O capillary), in 0, 24, and 48 h.

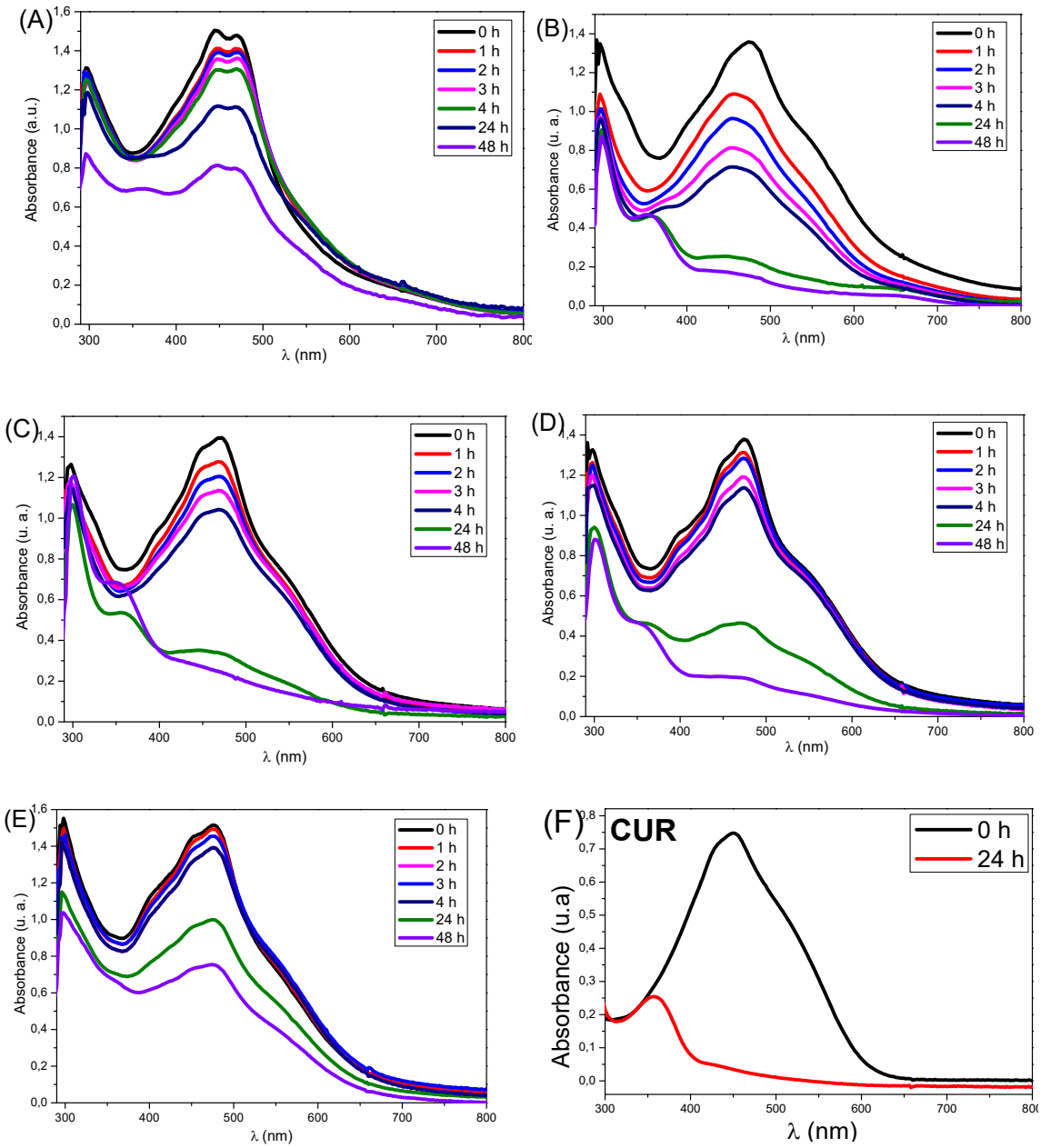

Figure S17. UV-vis spectra in /RPMI Culture medium (DMSO 0.5%) of the complexes (A) *A1*; (B) *A2*; (C) *A3*; (D) *A4*; (E) *A5* (40 μM) and (F) free curcumin (20 μM) at different times.

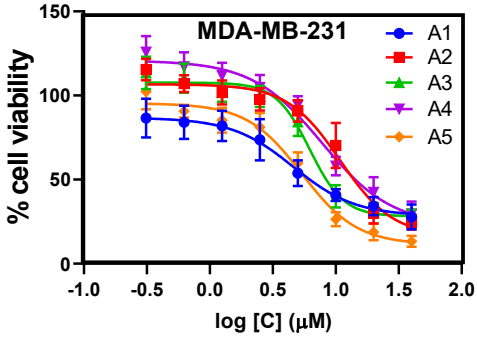
MDA-MB-231
A1
A2
A3
A4
A5
% cell viability
log [C] (µM)

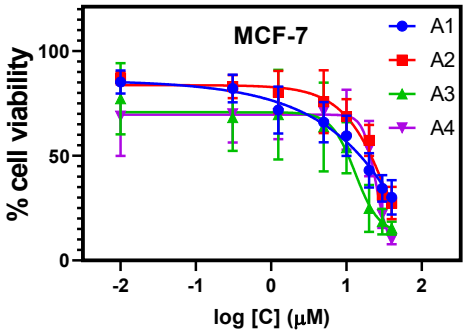
MCF-7
A1
A2
A3
A4
% cell viability
log [C] (µM)

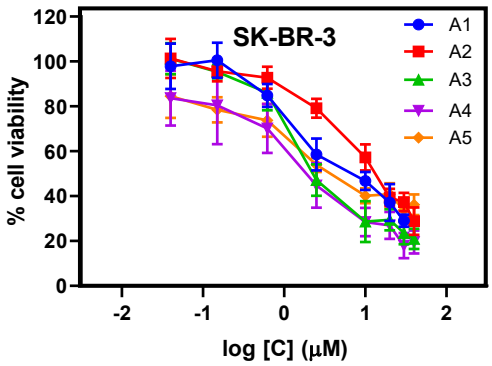
SK-BR-3
A1
A2
A3
A4
A5
% cell viability
log [C] (µM)

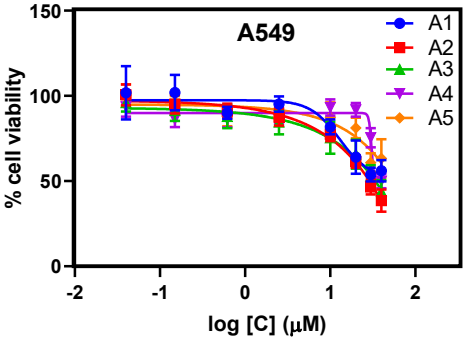
A549
A1
A2
A3
A4
A5
% cell viability
log [C] (µM)

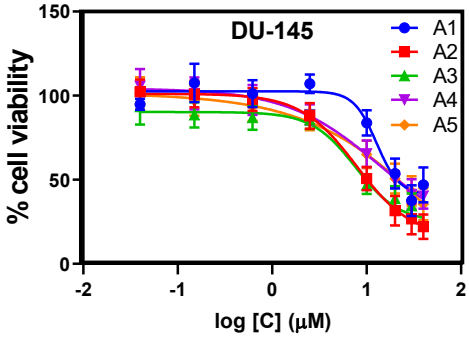
DU-145
A1
A2
A3
A4
A5
% cell viability
log [C] (µM)

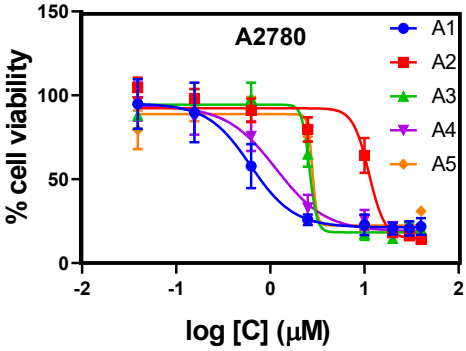
A2780
A1
A2
A3
A4
A5
% cell viability
log [C] (µM)

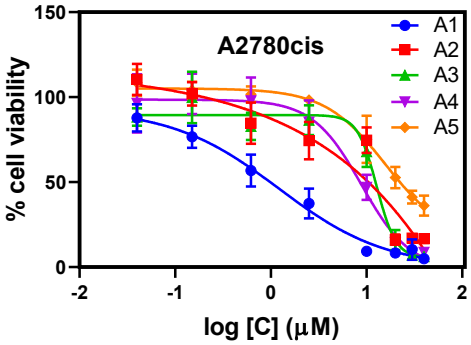
A2780cis
A1
A2
A3
A4
A5
% cell viability
log [C] (µM)

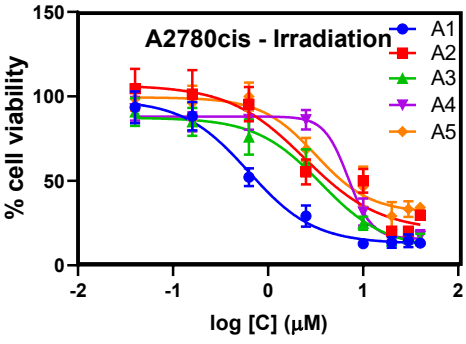
A2780cis - Irradiation
A1
A2
A3
A4
A5
% cell viability
log [C] (µM)

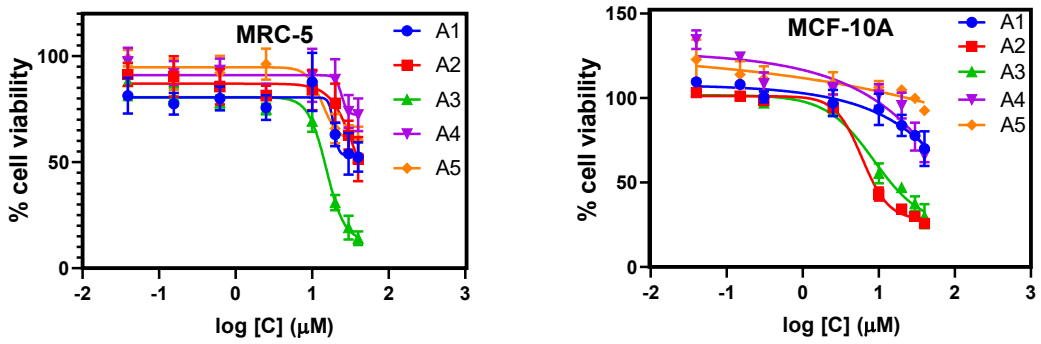

Figure S18. Cytotoxicity of complexes. Concentration-response curve of tumor cells (MDA-MB-231, MCF7, SKBR-3, A549, DU-145, A2780 and A2780cis) and non-tumor cells (MCF-10A and MRC-5) after complexes treatment for 48 h.

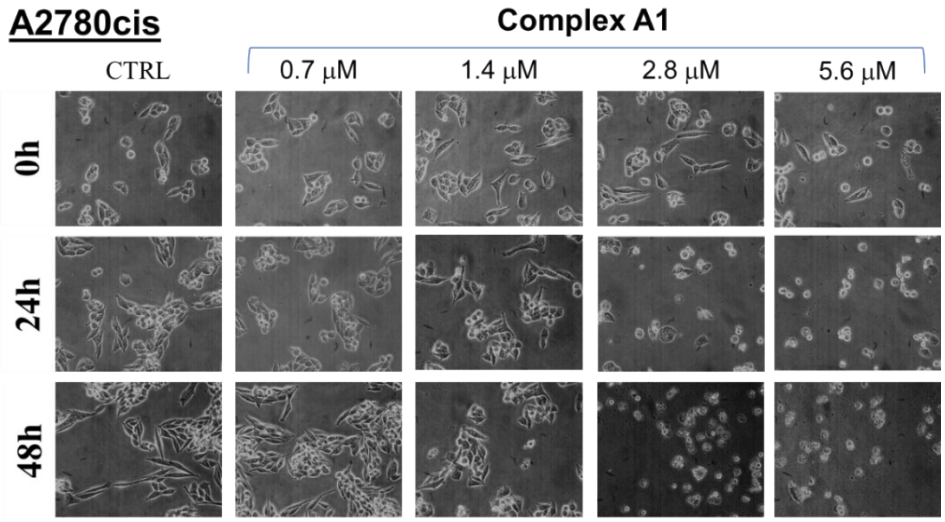

Figure S19. Effect of complex *A1* on A2780cis cell morphology after incubation for 0, 24, and 48 h.

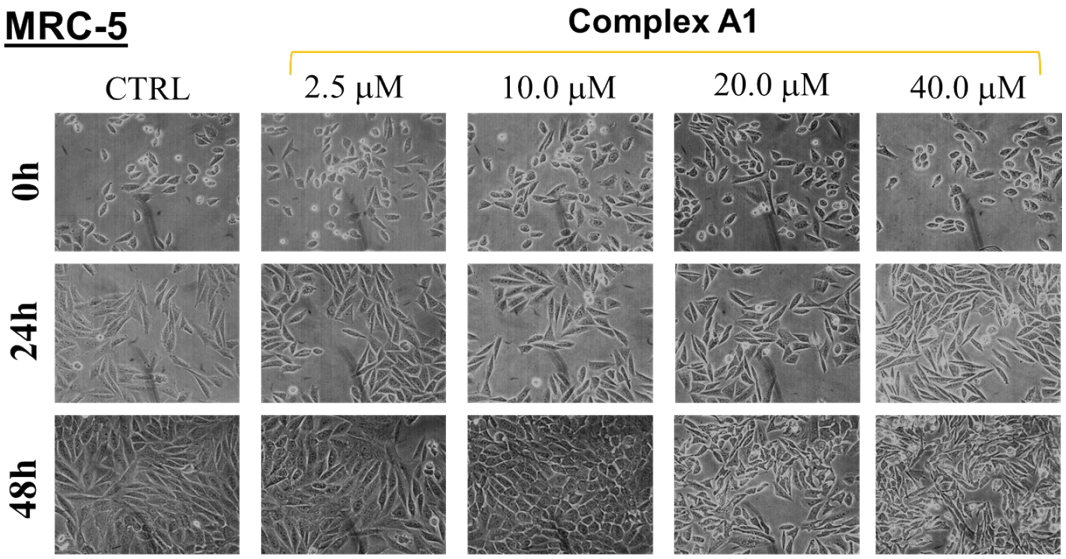

Figure S20. Effect of complex A1 on MRC-5 cell morphology after incubation for 0, 24, and 48 h.

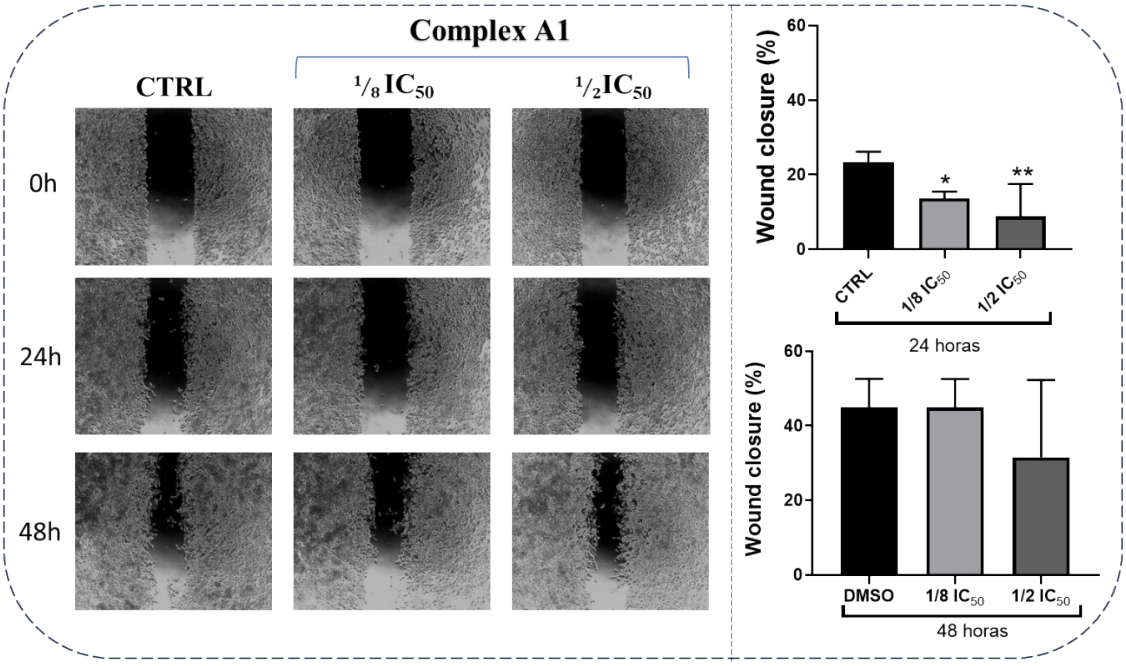

Figure S21. Effect of complex A1 on A2780cis cell migration by using an inverted microscope (4×) and graph of the wound-healing closure percentages for treatment with complex *A1*. These experiments were representative of three independent assays. Significance at (****) $p < 0.0001$ using ANOVA. Solvent control experiments were performed with DMSO (0.5%).

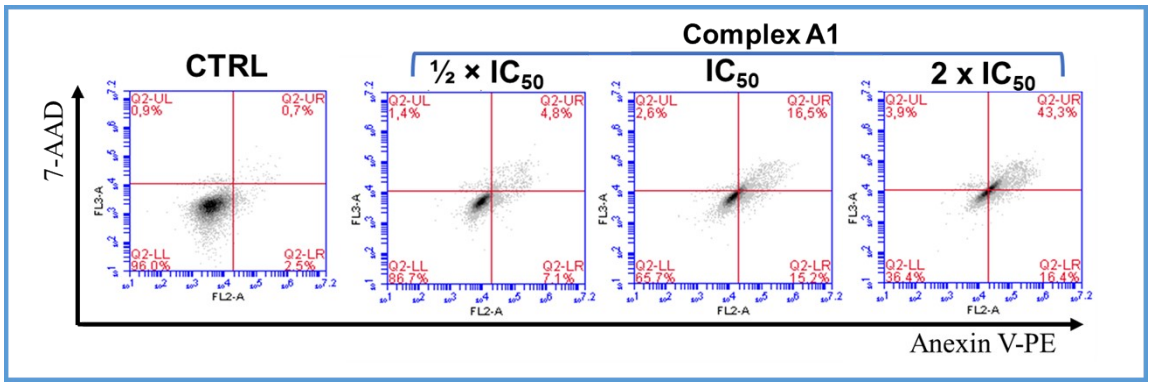

Figure S22. (A) Effects of complex A1 on apoptosis of A2780cis cells after 24 h of treatment at $^1/_2$ × IC_{50} (0.7 μM), IC_{50} (1.4 μM) and 2 × IC_{50} (2.8 μM) concentrations of complex A1. Apoptosis assay with PE-Annexin V (detected in the FL2-A channel) and 7AAD (detected in the FL3-A channel).

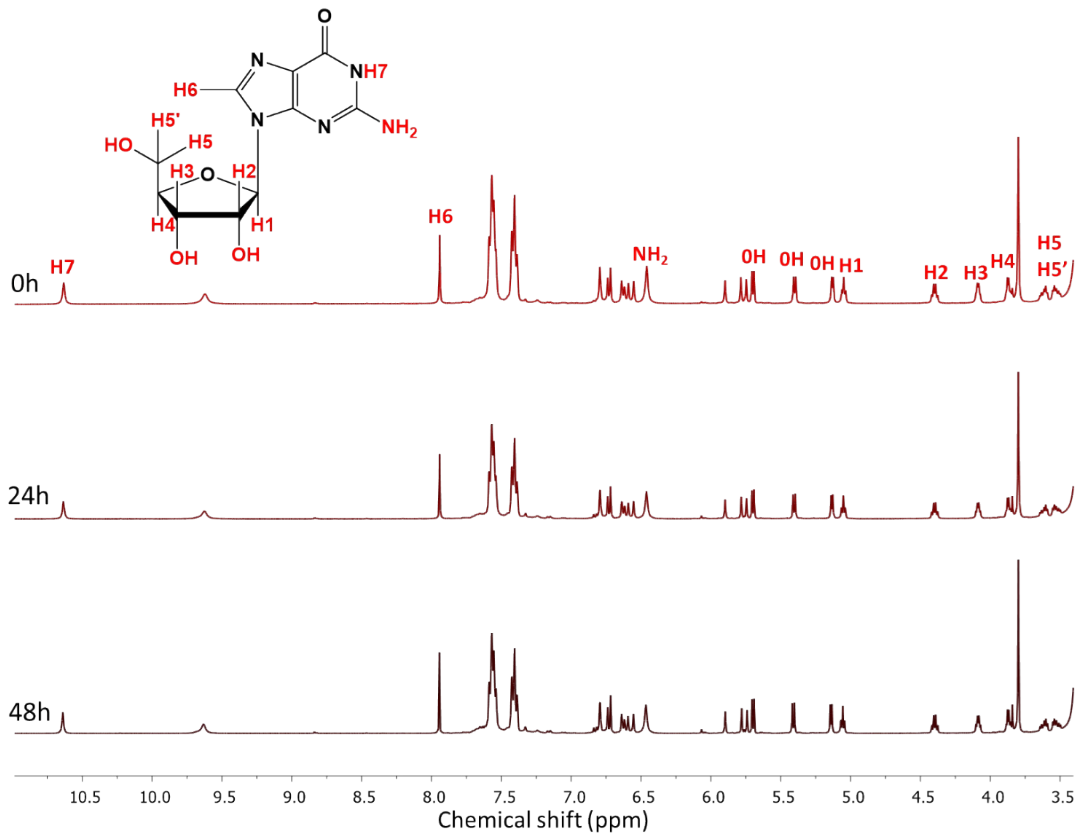

Figure S23. ^{1}H NMR spectra of the A1 complex with guanosine (1 mol: 2 mol) at 0, 24 and 48 hours in deuterated DMSO.

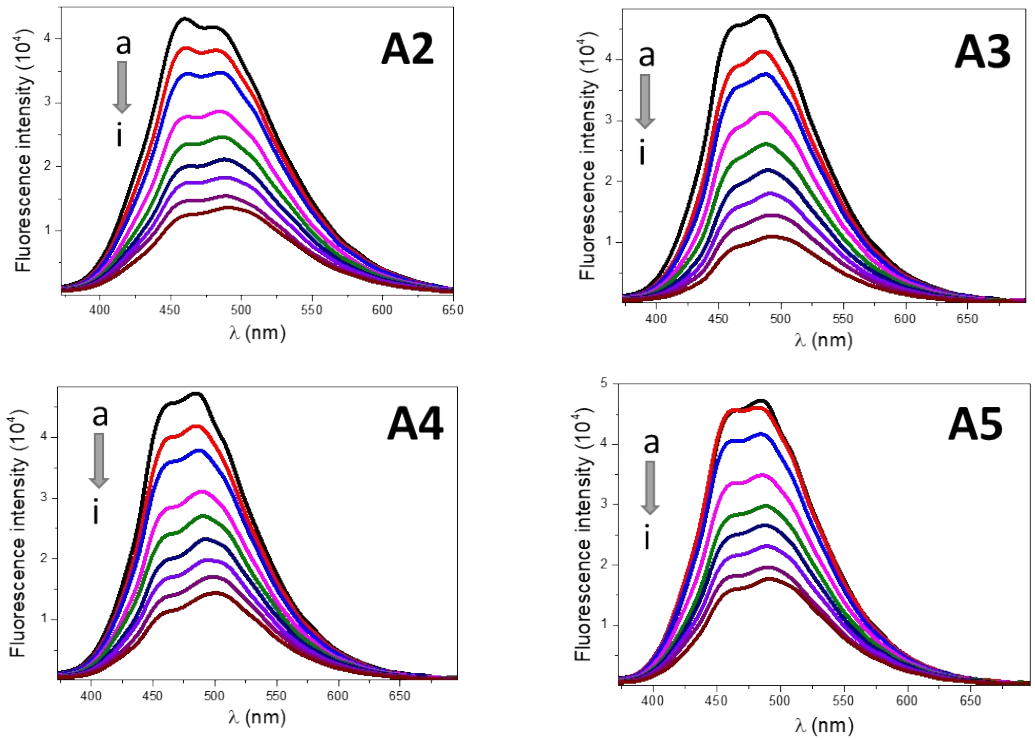

Figure S24. Emission spectra of Hoechst (2.5 μM)/CT-DNA (75 μM) (l_{ex} = 343 nm) with different concentrations of complexes A2-A5 (a= 0; b= 2.5 μM; c= 5.0 μM; d= 7.5 μM; e= 10.0 μM; f= 12.5 μM; g= 15.0 μM; h= 17.5 μM; i= 20.0 μM).

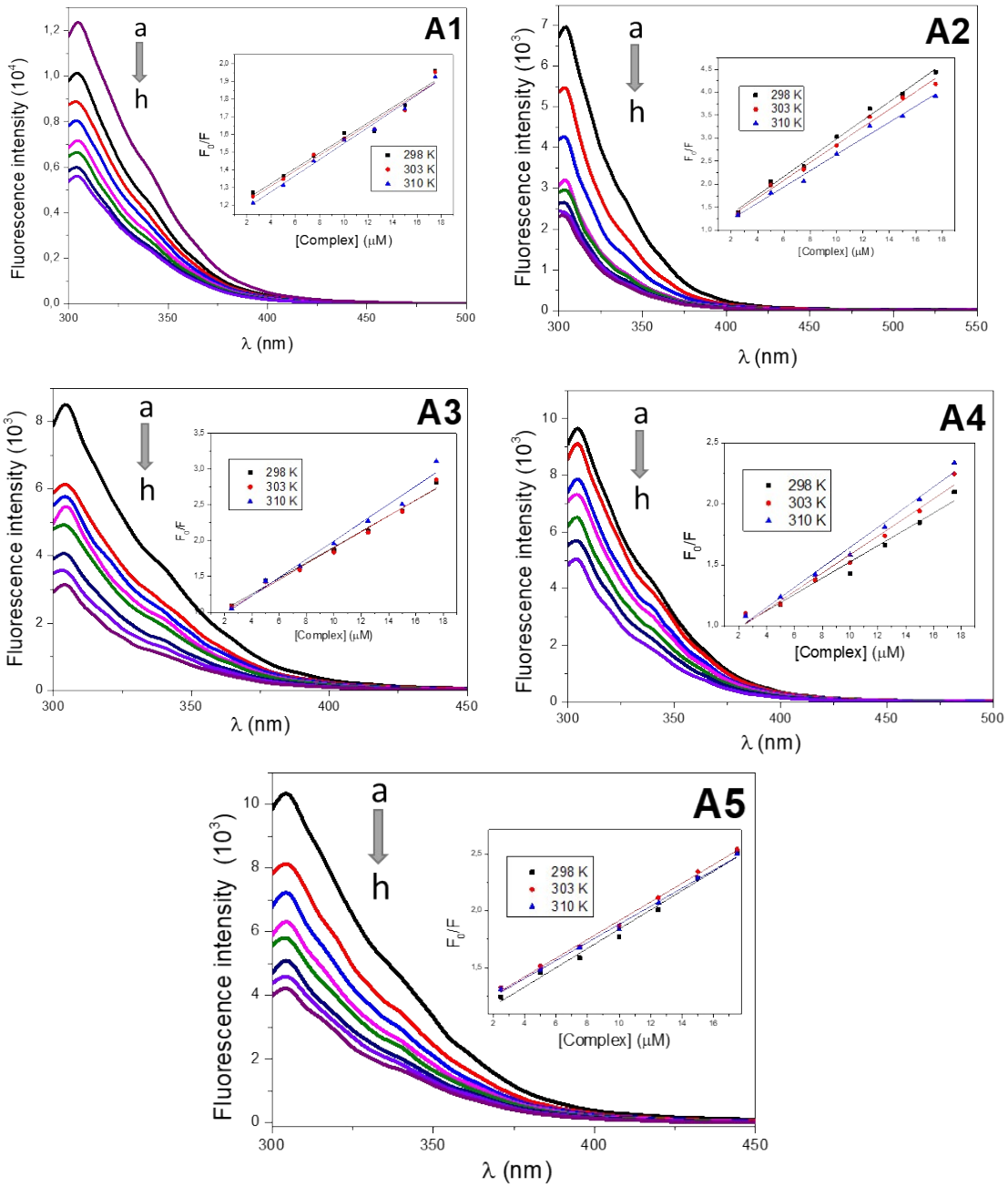

Figure S25. Fluorescence spectra of HSA solution (2.5 μM) in Tris–HCl buffer (0.1 M NaCl, pH 7,4) in the absence and presence of different concentrations of complexes A1-A5 (a = 0; b= 2.5 μM; c = 5.0 μM; d = 7.5 μM; e = 10.0 μM; f = 12.5 μM; g = 15.0 μM and h = 17.5 μM). Inset: Stern–Volmer plots for the quenching of HSA fluorescence by complexes, 298, 303 and 310 K.

Tables

Table S1. Selected Interatomic Distances and Bond Angles for complexes.

Bond lengths (Å)	Cur*	Complexes			
		A1	A2	A4	A5
Pd(1)–P(1)	–	2.2866(6)	2.2162(5)	2.2409(17)	2.2596(10)
Pd(1)–P(2)	–	2.2569(6)	2.2257(6)	2.2504(15)	2.2816(10)
Pd(1)–O(1)	–	2.0444(16)	2.0509(14)	2.063(4)	2.045(3)
Pd(1)–O(3)	–	2.0360(16)	2.0486(14)	2.051(4)	2.046(3)
C(1)–O(1)	1.298	1.286(3)	1.290(3)	1.285(7)	1.280(5)
C(3)–O(3)	1.303	1.285(3)	1.282(2)	1.271(7)	1.294(5)
bond angles (deg)		**Complexes**			
		A1	**A2**	**A4**	**A5**
O(1)–Pd(1)–P(1)		170.01(5)	176.25(4)	175.27(11)	177.49(8)
O(3)–Pd(1)–P(2)		178.18(5)	173.61(4)	176.92(12)	175.40(8)
P(2)–Pd(1)–P(1)		95.69(2)	86.01(2)	92.93(6)	95.95(4)
O(1)–Pd(1)–P(2)		87.14(5)	91.07(4)	90.87(11)	83.64(8)
O(3)–Pd(1)–P(1)		84.72(5)	89.30(4)	84.01(12)	88.63(8)
O(3)–Pd(1)–O(1)		92.74(6)	93.79(6)	92.21(15)	91.79(11)

*CCDC code 636155

Table S2. Crystal data and structure refinement parameters obtained for the complexes *A1*, *A2*, *A4* and *A5*.

	A1	**A2**	**A4**	**A5**
Empirical formula	$C_{57}H_{49}F_6O_6P_3Pd$	$C_{47}H_{43}F_6O_6P_3Pd$	$C_{49}H_{47}F_6O_6P_3Pd$	$C_{58}H_{50}Cl_9F_6FeO_6P_3Pd$
Formula weight	1143.27	1017.12	1045.17	1531.19
Temperature	100 K	100 K	293(2)	100(1)
Crystal system	Monoclinic	Monoclinic	Triclinic	Monoclinic
Space group	$P2_1/c$	$P2_1/n$	P-1	$P2_1/n$
Unit cell dimensions	a = 14.0442(3) Å b = 9.5822(2) Å c = 37.0985(7) Å α = 90° β = 94.609(2)° γ = 90°	a = 14.0940(2) Å b = 22.4280(3) Å c = 16.0300(3) Å α = 90° β = 112.924(2)° γ = 90°	a = 9.0366(6) Å b = 16.4302(12) Å c = 19.0475(13) Å α = 112.064(7)° β = 96.129(6)° γ = 101.480(6)°	a = 17.9737(3) Å b = 15.9310(3) Å c = 23.2031(5) Å α = 90° β = 95.1174(18)° γ = 90°
Volume/Å^3	4976.36(18)	4666.90(14)	2516.7(3)	6617.5(2)
Z	4	4	2	4
ρ_{calc}g/cm^3	1.526	1.448	1.379	1.537
μ/mm^{-1}	0.545	0.571	0.531	0.990
F(000)	2336.0	2072.0	1068.0	3080.0
Crystal size	0.188 × 0.062 × 0.027 mm^3	0.177 × 0.139 × 0.105 mm^3	0.208 × 0.102 × 0.063 mm^3	0.319 × 0.282 × 0.175 mm^3
2θ range for data collection	3.506 to 51.496°	3.742 to 51.5°	5.06 to 51.496°	4.354 to 51.36°
Index ranges	-16 ≤ h ≤ 17, -11 ≤ k ≤ 11, -45 ≤ l ≤ 45	-17 ≤ h ≤ 17, -27 ≤ k ≤ 27, -19 ≤ l ≤ 19	-11 ≤ h ≤ 11, -20 ≤ k ≤ 20, -23 ≤ l ≤ 23	-21 ≤ h ≤ 21, -18 ≤ k ≤ 19, -28 ≤ l ≤ 28
Reflections collected	76902	94656	47990	57867
Independent reflections	9514 [R_{int} = 0.0650, R_{sigma} = 0.0336]	8938 [R_{int} = 0.0472, R_{sigma} = 0.0211]	9594 [R_{int} = 0.1055, R_{sigma} = 0.0941]	12522 [R_{int} = 0.0429, R_{sigma} = 0.0325]
Data/restraints/parameters	9514/0/662	8938/0/572	9594/151/590	12522/84/797
Goodness-of-fit on F^2	1.081	1.058	1.004	1.105
Final R indexes [I>=2σ (I)]	R_1 = 0.0339, wR_2 = 0.0765	R_1 = 0.0277, wR_2 = 0.0685	R_1 = 0.0800, wR_2 = 0.2250	R_1 = 0.0473, wR_2 = 0.1074
Final R indexes [all data]	R_1 = 0.0395, wR_2 = 0.0789	R_1 = 0.0328, wR_2 = 0.0722	R_1 = 0.1093, wR_2 = 0.2609	R_1 = 0.0691, wR_2 = 0.1247
Largest diff. peak/hole	0.74/-0.62 e.Å^{-3}	0.65/-0.48 e.Å^{-3}	2.06/-1.41 e.Å^{-3}	1.11/-1.11 e.Å^{-3}

Table S3. Assign the main IR bands of free curcumin and complexes.

	Vibrational Frequency (cm^{-1})					
	Compounds					
	Cur	**A1**	**A2**	**A3**	**A4**	**A5**
ν OH	3448	3503	3510	3458	3514	3491
ν (C=O) ketone	1628	1621	1624	1616	1622	1620
ν (C=C) aliphatic	1514	1504	1504	1504	1506	1504
ν (C–O) phenol	1282	1282	1280	1290	1292	1288
ν P–C	-	1095	1030	1085	1100	1095
ν P–F	-	840	840	844	840	844

Table S4. In vitro cell viability results (IC_{50} values) toward some cell lines studied.

Compounds	**IC_{50} (μmol/L) 48 h**				
	MDA-MB-231	**MCF-7**	**SKBR-3**	**A2780**	**A2780cis**
P1 - $[PdCl_2(PPh_3)_2]$	≥25	≥25	≥25	n.t	≥25
P2 - $[PdCl_2(dppe)]$	≥50	≥50	≥50	≥50	≥50
P3 - $[PdCl_2(dppp)]$	≥50	≥50	≥50	n.t	≥50
P4 - $[PdCl_2(dppb)]$	≥25	≥25	≥25	n.t	≥25
P5 - $[PdCl_2(dppf)]$	≥50	≥40	≥40	n.t	9.9 ± 0.9

Table S5 - In vitro cell viability results (IC_{50} values) toward some cell lines studied.

Compounds	**IC_{50} (μM) 48 h**		
	MCF-7	**A549**	**DU-145**
A1 - $[Pd(cur)(PPh_3)_2]PF_6$	24.8 ± 0.2	≥40	12.6 ± 0.4
A2 - $[Pd(cur)(dppe)]PF_6$	22.6 ± 0.3	≥40	18.6 ± 0.4
A3 - $[Pd(cur)(dppp)]PF_6$	12.0 ± 1.1	≥40	18.5 ± 1.3
A4 - $[Pd(cur)(dppb)]PF_6$	15.1 ± 0.4	≥40	22.9 ± 0.6
A5 - $[Pd(cur)(dppf)]PF_6$	≥40	≥40	≥40
Curcumin	36.8 ± 1.6	38.9 ± 1.3	n.t
Cisplatin	13.9 ± 2.0	14.4 ± 1.4	2.3 ± 0.4